

**Contributions of Fuel Combustion to  
Pollution by Airborne Particles in  
Urban and Non-Urban Environments**

**An ERDC Study**

**Final Report**

**Vol I**

by

**Australian Nuclear Science and  
Technology Organisation**

**New South Wales Environment Protection  
Authority**

**Pacific Power Corporation**

**University of New South Wales**

**Macquarie University**

**June 1995**



**Contributions of Fuel Combustion to  
Pollution by Airborne Particles in  
Urban and Non-Urban Environments**

**An ERDC Study**

**Final Report**

**Vol I**

by

**Australian Nuclear Science and  
Technology Organisation**

**New South Wales Environment Protection  
Authority**

**Pacific Power Corporation**

**University of New South Wales**

**Macquarie University**

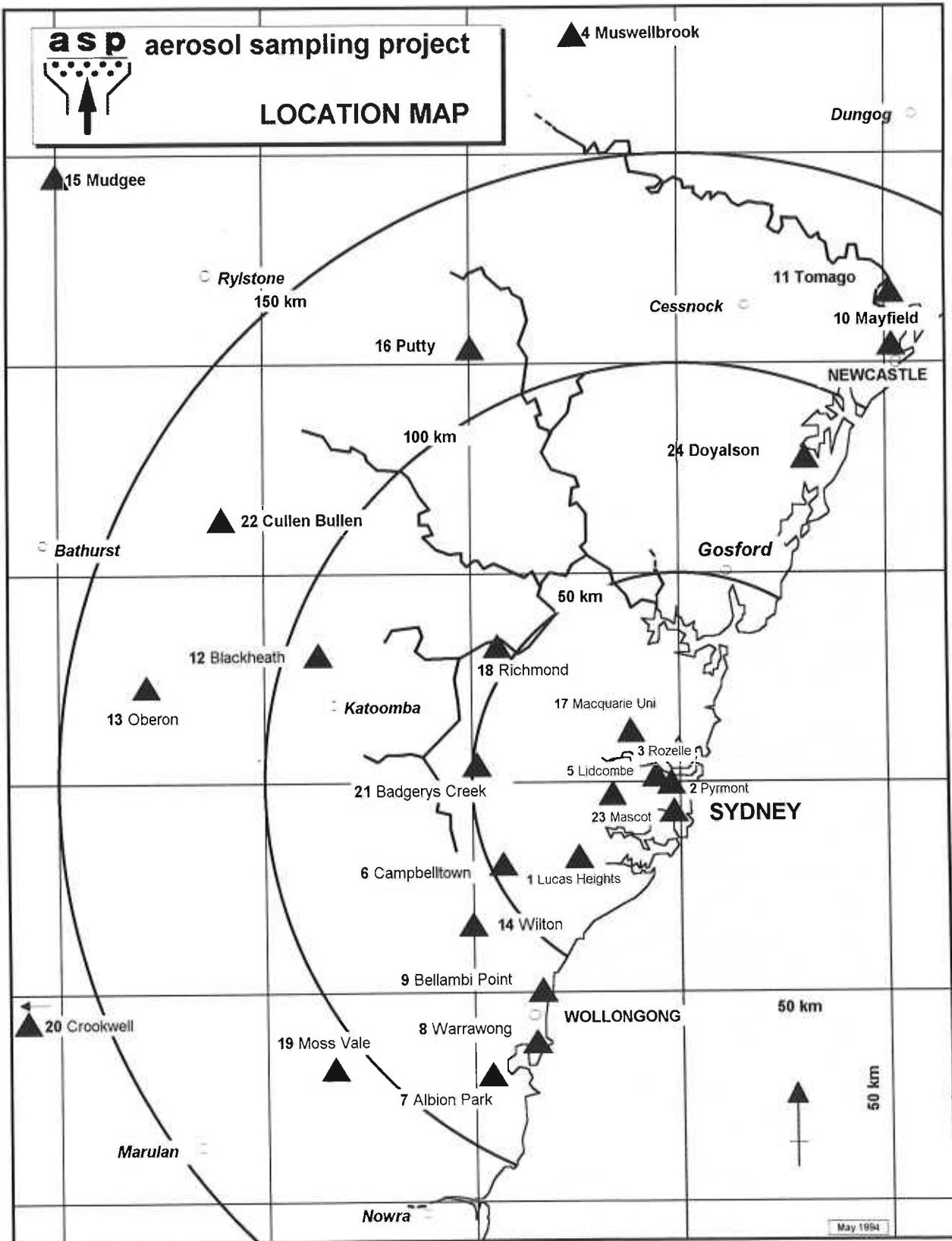
**June 1995**



**asp aerosol sampling project**



**LOCATION MAP**





## EXECUTIVE SUMMARY

The project was funded by the Energy Research Development Corporation (ERDC) and was a collaborative investigation involving the Australian Nuclear Science and Technology Organisation (ANSTO), the New South Wales Environmental Protection Authority (NSW EPA), Pacific Power, The University of New South Wales and Macquarie University.

The objectives of the study were:

- To establish a fine particle monitoring network covering the greater Wollongong/Sydney/Newcastle areas
- To investigate the relationships between fuel combustion and fine particle aerosols in urban and non urban environments
- To add to the limited database of baseline information on concentrations of fine particles resulting from such processes as fossil fuel burning, and industrial manufacturing
- To identify and quantify sources of fine particles in New South Wales
- To introduce into Australia accelerator based Ion Beam Analysis (IBA) techniques for the analysis of filter papers obtained from large scale monitoring networks.

To achieve these objectives a network of 25 sampling units was established to collect fine airborne particles with aerodynamic diameter less than  $2.5\mu\text{m}$  (PM<sub>2.5</sub>). The network covered over 60,000 square kilometres of NSW and extended from Newcastle, Sydney and Wollongong to a distance of 200 km inland. One of the sampling units was installed at Cape Grim in northwest Tasmania to measure natural background particle concentrations.

The project commenced in January 1991; the sampling network was installed during 1991 and operated successfully with an overall collection efficiency greater than 97% over the eighteen month period between January 1992 and June 1993. During the project, ion beam analysis techniques were used to analyses over 5000 filters from the

network for 25 different elements. As a result of the investigation a data base of over 150,000 measurements has been established.

For the study, elements have been combined into a few major components to represent major constituents of the aerosols, which in conjunction with some tracer elements these have been used to 'fingerprint' important sources. These parameters include: the total fine particle mass, ammonium sulphate, 'organic matter', 'soil', 'soot' and elements such as potassium, iron, copper, zinc, copper, bromine and lead. The trace element potassium is indicative of smoke from wood burning, combustion processes and bushfires; iron and copper can be used to identify industrial processes such as metal smelting and steel manufacturing, while lead and bromine can be used as a tracer for motor vehicles and industry.

The average composition of fine particles collected by the ERDC project across the network was 23% 'organic matter', 23% 'ammonium sulphate' 22% elemental carbon (soot), 7% 'salt', 6% 'soil' and 1% lead. The remainder comprised nitrates, trace elements and water. There were significant seasonal variations in fine aerosol composition across the network but, on average, three quarters of the aerosols resulted from anthropogenic activities. In 1992 the maximum yearly average total mass occurred at Mayfield  $12.2\mu\text{g}/\text{m}^3$ , while the average across all sites in the network was  $7.7\mu\text{g}/\text{m}^3$ .

**Lead** in the fine particle form is derived largely from the combustion of leaded petrol. The highest yearly average concentration of lead occurred at Mascot ( $0.33\mu\text{g}/\text{m}^3$ ), while the highest 24 hour concentration of lead ( $1.74\mu\text{g}/\text{m}^3$ ) was measured at Lidcombe. There were lower concentrations of fine particle lead in the industrial suburbs of Warrawong and Mayfield than in the inner Sydney suburbs. Concentrations of fine particle lead decreased rapidly with distance from Sydney, being reduced by a factor of 20 between the centre of Sydney and rural areas 200 km inland. Lead concentrations showed strong seasonal variations, being 10 times higher in winter than in summer for inner Sydney sites.

**Elemental Carbon** (soot particles) is derived from incomplete combustion processes such as occur in motor vehicles, burning of fossil fuel and bushfires, and the occurrence of 'soot' was widespread. Large seasonal variations were observed with winter concentrations being 2 to 6 times higher than the summer values. The three highest

## EXECUTIVE SUMMARY

yearly average concentrations occurred at Mascot ( $4.2\mu\text{g}/\text{m}^3$ ), Pyrmont( $3.9\mu\text{g}/\text{m}^3$ ) and Mayfield( $\mu\text{g}/\text{m}^3$ ).

**'Organic matter'** (compounds containing carbon, hydrogen and oxygen) was estimated to be one of the most abundant species in the urban atmosphere. It is produced by motor vehicles, fossil fuel combustion, incineration, vegetation burning and industrial processes. There were strong seasonal variations in concentrations at all sites with winter values being typically 3 to 5 times the summer concentrations. The maximum yearly average concentration ( $3.6\mu\text{g}/\text{m}^3$ ) was recorded at Cullen Bullen. The next highest average values were measured in Sydney at Mascot( $3.1\mu\text{g}/\text{m}^3$ ), Rozelle( $3.0\mu\text{g}/\text{m}^3$ ), Pyrmont( $2.9\mu\text{g}/\text{m}^3$ ) and Lidcombe( $2.6\mu\text{g}/\text{m}^3$ ).

**'Ammonium sulphate'** Sulphur dioxide emitted during fossil fuel combustion and smelting processes may be slowly oxidised to sulphuric acid and then be neutralised by naturally occurring ammonia in the atmosphere to form ammonium hydrogen sulphate. The highest yearly average concentration occurred at Warrawong ( $2.7\mu\text{g}/\text{m}^3$ ), followed by Pyrmont ( $2.4\mu\text{g}/\text{m}^3$ ), Muswellbrook ( $2.4\mu\text{g}/\text{m}^3$ ), Mayfield ( $2.3\mu\text{g}/\text{m}^3$ ) and Rozelle ( $2.1\mu\text{g}/\text{m}^3$ ). There were strong seasonal variations in concentrations with summer values being 2 to 5 times higher than the winter values at most sites. The highest seasonal variations were found at sites remote from the industrial/urban centres of Newcastle, Sydney and Wollongong.

**'Salt'**, as sodium chloride, was highest at the coastal sites as a result of sea spray. Depending on wind directions, concentrations 200 km inland were typically 75% lower than concentrations measured at the coast. 'Salt' concentrations in summer were generally 2 to 10 times higher than in winter reflecting the higher frequency of onshore winds in the warmer months of the year. The maximum yearly average 'salt' concentration occurred at the baseline station at Cape Grim an northwest Tasmania ( $2.2\mu\text{g}/\text{m}^3$ ). The next highest average concentration was measured at Bellambi north of Wollongong ( $1.8\mu\text{g}/\text{m}^3$ ).

**'Soil'** is largely inorganic and comprised of complex minerals containing magnesium, aluminium, silicon, calcium, potassium, titanium and iron. It is introduced into the air as a result of strong winds, motor vehicle movements, agricultural practice and industrial and mining activities. Fly ash from combustion processes has a similar composition to 'soil'. The highest yearly average 'soil' concentration was measured at Mayfield ( $1.6\mu\text{g}/\text{m}^3$ ).

## EXECUTIVE SUMMARY

This value is 60% higher than the value measured in the industrial area at Warrawong in the Wollongong region, and nearly 3 times the concentrations measured at Mascot.

**'Smoke'** Fine potassium is used as an indicator for smoke from the combustion of vegetation such as wood burning and bush fires. There were considerable seasonal variations in concentrations of 'smoke' across the network, with monthly average concentrations being about twice as high in winter as in summer. At some sites, for example Rozelle, Macquarie University, Richmond and Cullen Bullen average winter smoke levels (50-65 ng/m<sup>3</sup>) were 3 to 6 times higher than the summer values. In 1992, the average monthly smoke concentration across the network was 22 ng/m<sup>3</sup>.

The objectives of the project have been addressed. Some sources of fine particles have been identified and quantified, and some relationships between fuel combustion and fine aerosols have been established. The scope of further work in these two areas is large, and further analysis of the data acquired will more fully quantify relationships between natural and anthropogenic fine particle sources.

## TABLE OF CONTENTS

EXECUTIVE SUMMARY .....	i
TABLE OF CONTENTS .....	v
LIST OF TABLES .....	ix
LIST OF FIGURES .....	xii
GLOSSARY .....	xix
1. INTRODUCTION .....	1
1.1 HISTORY OF ASP .....	1
1.2 PROJECT OBJECTIVES .....	3
1.3 THE SCOPE OF THE ERDC STUDY .....	3
1.4 PREVIOUS PARTICLE STUDIES IN THE ERDC PROJECT AREA .....	4
2. SOURCES AND CHARACTERISTICS OF AEROSOLS .....	6
2.1 SOURCES OF AIRBORNE PARTICLES .....	7
2.2 CHARACTERISTICS OF AIRBORNE PARTICLES .....	9
2.3 POLLUTION GUIDELINES OR GOALS .....	12
3. THE AEROSOL SAMPLING NETWORK .....	15
3.1 SITE LOCATIONS .....	15
3.2 DESCRIPTION OF SAMPLING OPERATIONS .....	17
3.2.1 The Sampling Unit .....	17
3.2.1 The Filter .....	17
3.2.3 Sampler Calibrations .....	18
4. ANALYSIS TECHNIQUES .....	20

## TABLE OF CONTENTS

4.1 ION BEAM ANALYSIS (IBA) TECHNIQUES .....	20
4.1.1 Particle Induce X-ray Emission (PIXE) .....	21
4.1.2 Particle Induced Gamma-ray Emission (PIGME) .....	24
4.1.3 Particle Elastic Scattering (PESA) .....	25
4.1.4 Rutherford Backscattering (RBS) .....	26
4.1.5 Laser Integrated Plate Methods (LIPM) .....	28
4.1.6 Minimum Detectable Limits (MDL) and Errors .....	32
4.2 FILTERS .....	35
4.2.1 Filter Weighing .....	35
4.3 PSEUDO ELEMENTS AND COMPOSITE VARIABLES .....	36
4.3.1 Sulphate .....	37
4.3.2 'Salt' .....	41
4.3.3 'Soil' .....	41
4.3.4 'Smoke' .....	42
4.3.5 'Organic Matter' .....	43
4.3.6 Reconstructed Mass (RCM) .....	44
4.4 QUALITY ASSURANCE .....	45
4.4.1 Error Codes .....	45
4.4.2 Ion Chromatography (IC) .....	46
4.4.3 Neutron Activation Analysis (NAA) .....	48
5. RESULTS AND DATA INTERPRETATION .....	50
5.1 THE ERDC PROJECT DATABASE .....	50

## TABLE OF CONTENTS

5.2 METHODS OF DATA ANALYSIS AND PRESENTATION .....	51
5.2.1 Analysis of filter .....	51
5.2.2 Elemental composition of filters by site .....	51
5.2.3 Elemental composition by region .....	52
5.3 DISCUSSION OF RESULTS .....	52
5.3.1 Annual average concentrations of elements .....	53
5.3.2 Fine particle concentrations in the ASP study sectors .....	55
5.3.3 Seasonal variations .....	63
5.3.4 Urban, non-urban and rural differences .....	64
5.4 DISCUSSION OF FINE PARTICLE COMPONENTS .....	64
5.4.1 Total fine particle mass .....	64
5.4.2 'Soil' .....	65
5.4.3 Sulphur .....	66
5.4.4 Lead .....	66
5.4.5 Smoke .....	69
5.4.6 Iron .....	71
5.4.7 Zinc .....	72
5.4.8 'Organic matter' (compounds containing carbon, hydrogen and oxygen) .....	72
5.4.9 Sea 'salt' .....	72
5.4.10 'Soot' .....	72
5.5 ELEMENT RATIOS AS INDUSTRIAL INDICATORS .....	73
5.5.1 Cobalt / iron .....	73

TABLE OF CONTENTS

5.5.2 Vanadium / carbon .....	73
5.5.3 Iron / sulphur .....	73
6. CONCLUSIONS .....	74
7. RECOMMENDATIONS .....	78
8. ACKNOWLEDGEMENTS .....	79
9. REFERENCES .....	80
10. PUBLICATIONS .....	91
APPENDIX A. ADDITIONAL INFORMATION .....	92
A.1 THE EFFECT OF FINE PARTICLES ON VISIBILITY .....	92
A.2 FINE PARTICLES AND HEALTH EFFECTS .....	94
A.2.2 Health Effects .....	94
A.3 CLIMATE EFFECTS .....	96
APPENDIX 1	
Volume 2 Daily data for January - June 1992	
Volume 3 Daily data for July - December 1992	
Volume 4 Daily data for January - June 1993	
APPENDIX 2	
Volume 5 Monthly data for January 1992 - June 1993	

## LIST OF TABLES

**Table 2.1.** Uses and common elemental signatures for (a) fuel combustion sources, (b) industrial processes and (c) naturally occurring particle sources.

**Table 2.2.** Particle size ranges for a series of commonly occurring aerosols.

**Table 2.3.** Ambient air quality standards for California and the USA

**Table 2.4.** Ambient air quality objectives for New South Wales as adapted from various US EPA and NH&MRC goals.

**Table 3.1.** Classification of the 25 sampling sites for the ERDC project.

**Table 4.1.** Comparison of the measured PIXE values with the nominal values for six Micromatter standard filters for each month in 1992.

**Table 4.2.** The absorption efficiency  $\varepsilon_{ap}$  and scattering efficiency  $\varepsilon_{sp}$  for various components of the fine mass for 2 days in January 1988 in Denver, USA, taken from the work of Sloane et al 1991.

**Table 4.3.** Summary of the steps used in standard thermal optical reflectance (TOR) measurements, after Eldred 1993.

**Table 4.4.** Typical experimental errors for all analysis techniques used in the ERDC network during 1992.

**Table 4.5.** Typical statistical counting errors associated with the elemental analysis of 1000 filters obtained from the ERDC network during 1992.

**Table 4.6.** The definition of pseudo elements SO<sub>4</sub>, NHSO<sub>4</sub>, NHSO<sub>4</sub>bi and HSO<sub>4</sub> from the elemental sulphur measurement.

**Table 4.7.** Error codes that are carried with each filter analysed.

## LIST OF TABLES

**Table 5.1** Species measured and stored in the chemical data base.

**Table 5.2.** Average concentrations of elements and pseudoelements in the air collected at all sites in the network throughout 1992. Standard deviations for the 25 sites are also given.

**Table 5.3.** Average conditions under which filters were collected. Standard deviations for the 25 sites are also given.

**Table 5.4.** Average elemental composition of particles collected on the filters at all sites in the network throughout 1992, expressed as a percentage of the total fine particle mass.

**Table 5.5.** Ranking of sites in terms of the concentrations of major aerosol components and indicator elements. Values are average concentrations recorded during 1992 in  $\text{ng/m}^3$ .

**Table 5.6.** Sampling sites allocated to the sectors 0, 0-25, 25-50, 50-100, 100-200, km from the Sydney Central Business District (SCBD), and to the Wollongong and Newcastle sectors. Cape Grim (Tasmania) is a global baseline monitoring station.

**Table 5.7.** Annual average ratios of (TSP/PM<sub>2.5</sub>), for Pb and Fe during 1992 at Mayfield Rozelle and Warrawong. Standard deviations are given after each value.

**Table 5.8.** Average values for total fine mass, hydrogen, potassium, elemental carbon, organic matter and smoke for the four sites at Campbelltown (ASP6), Bellambi (ASP9), Wilton (ASP14) and Richmond (ASP18) during bushfires on 23 August 1992.

**Table 5.9.** Comparison of the summer and winter average monthly smoke values for the sampling sites at Rozelle, Macquarie University, Richmond and Cullen Bullen during 1992 and 1993.

**Table 6.1** Average concentrations of elements for PM<sub>2.5</sub> particles for all sites in the network, 1992

**Table 6.2** The five sites with the highest and lowest yearly average concentrations for major fine particle components.

LIST OF TABLES

**Table A.1.** Typical scattering and absorption coefficients ( $\mu\text{m}^{-1}$ ) for fine aerosols in USA. Adapted from Groblicki et al 1981 and Appel et al 1985.

## LIST OF FIGURES

**Figure 2.1.** Dry removal rate (arbitrary units) for atmospheric aerosols versus particle diameter showing the two main mechanisms for aerosol removal from the atmosphere.

**Figure 2.2.** Bimodal particle mass distribution as a function of particle diameter. Adapted from the work of Hopke 1985.

**Figure 2.3.** Particle size fractions versus particle size for (a) aerosols from plumes from a power station, (b) aerosols from a manganese smelter. Adapted from the work of Kim et al 1989.

**Figure 3.1** Location map of the 24 ERDC fine particle aerosol samplers within 200 km of the city of Sydney. The coal fired power stations serving the Sydney area are also shown.

**Figure 3.2.** A photograph of a standard ASP sampling unit and pump. The unit was designed and built at ANSTO.

**Figure 3.3** Schematic diagram of an ASP Cyclone Sampling Unit. Air is pulled through the stack into the cyclone by the pump at 22 L/min for 24 hours. The Magnehelic and vacuum gauges are used to monitor this flow rate. The 7 day timer turns the pump on, every Wednesdays and Sunday.

**Figure 3.4.** A schematic diagram of a mounted sampler and its pump housing.

**Figure 3.5.** A schematic diagram of the air flow system through an ASP sampling unit.

**Figure 3.6.** The 50% size selective cutoff versus flow rate for the cyclone system used in the ASP network (John and Reischl 1980). The system is designed for 2.5  $\mu\text{m}$  diameter particles at 21.7 L/min flow rate.

**Figure 3.7.** A photograph of the 'Tupperware' box and its contents, used for mailing the filter cassettes around NSW.

**Figure 3.8.** The collection and analysis efficiency for all filters for all reasons for the 12 months during 1992.

## LIST OF FIGURES

**Figure 3.9.** Calibration curve for the flow rate through the critical orifice as measured by a calibrated rotameter versus the Magnehelic gauge reading for the ASP sampler at Lucas Heights.

**Figure 3.10.** Calibration curve for the flow rate through the critical orifice as measured by a calibrated rotameter versus the vacuum gauge reading for the ASP sampler at Lucas Heights.

**Figure 4.1.** Ion beam interactions with solid targets. The ion beam penetrates the target surface interacting with the target atoms as it loses energy.

**Figure 4.2.** Typical PIXE spectra for (a) Mascot (ASP23) an inner Sydney site and (b) Oberon a rural site on 24 June 1992. The solid curve is the fit to the experimental data (dashed curve) using the computer codes at ANSTO (Clayton 1986).

**Figure 4.3.** The number of X-rays for each ( $\mu\text{g}/\text{cm}^2$ ) of elemental material on the filter per 3  $\mu\text{C}$  run on our accelerators for each element in the periodic table from aluminium to uranium.

**Figure 4.4.** A typical PIGME spectrum for a filter from the Cape Grim (ASP25) site in north western Tasmania for the 16 August 1992. This spectrum was obtained simultaneously with the equivalent PIXE spectrum using 2.6 MeV protons and a total accelerator run time of just a few minutes (3  $\mu\text{C}$  of charge). The lower plot is a blow up of the region from 0 to 700 keV showing the Na 440 keV gamma ray in more detail.

**Figure 4.5.** Schematic of a typical PESA set up for a thin aerosol filter sample for 2.6 MeV protons. The protons scatter off the hydrogen atoms in the sample and are detected at  $30^\circ$ . The lower plot is an idealised PESA spectrum described in the text.

**Figure 4.6.** Typical PESA spectra for Mascot (ASP23) and Cape Grim (ASP25) taken on 24 June 1992. The hydrogen peaks are well separated from the peaks due to other heavier elements making its analysis from such a spectrum simple.

**Figure 4.7.** Typical RBS spectrum obtained for Teflon filter, showing the carbon, nitrogen, oxygen and fluorine peaks. The run conditions are the standard IBA conditions for 2.6 MeV protons with the detector set at a scattering angle of  $169^\circ$ .

## LIST OF FIGURES

**Figure 4.8.** Schematic diagram of the laser integrated plate method (LIPM). The laser is a HeNe laser with 633nm wavelength.

**Figure 4.9.** The layered correction R as a function of filter fine particle loading. The average loading for 1992 was  $107 \mu\text{g}/\text{m}^3$  giving  $R=0.50$ .

**Figure 4.10.** Minimum detectable limits for the analysis techniques used in the ERDC project

**Figure 4.11.** The weight of a standard 20 mg weight versus time using the Metler micro-balance. The mean value over the period June to December 1992 was  $(20.0062 \pm 0.0015)$  mg.

**Figure 4.12.** Vacuum test on filters before and after IBA analysis, showing that the fine particle mass varies by less than 8% in vacuum, returning to normal in less than 48 hrs after removal from vacuum. The top plot is for 10 filters with average mass loadings ( $210 \mu\text{g}$ ) and the bottom plot is for heavily loaded filters ( $265 \mu\text{g}$ ). The solid line is the mean with no temperature or humidity corrections and the dashed line is the corrected mean. The standard deviations for each point in time (SD) are shown on the plots.

**Figure 4.13.** Correlation of sulphur with nitrogen at Muswellbrook during 1993: all months (a), summer months (b) and winter months (c).

**Figure 4.14.** Correlation of sulphur with nitrogen at all sites during December 1992.

**Figure 4.15.** Sulphur versus hydrogen data for all sites in the ERDC network for 1992. The solid lines represent the expected ratios for ammonium sulphate, and sulphuric acid aerosols.

**Figure 4.16.** Reconstructed mass [equ.(4.9)] versus the gravimetric mass for all ERDC sites for 1992.

**Figure 4.17.** PIXE analysis versus ion chromatography results for (a) sulphur and (b) chlorine. The sulphur results are compared with the  $\text{SO}_4^{2-}$  ion concentrations and hence are expected to differ from the PIXE concentrations by a factor of (1/3).

## LIST OF FIGURES

**Figure 4.18.** Ion chromatography results versus gravimetric mass for (a) nitrate ions and (b) fluoride ions. The MDLs for nitrate ( $150 \text{ ng/m}^3$ ) and fluoride ions ( $60 \text{ ng/m}^3$ ) are shown as horizontal lines on the plots.

**Figure 4.19.** The PIXE/ PIGME techniques versus neutron activation analysis (NAA) for 14 elements measured on 100 filters during 1992.

**Figure 4.20.** The PIXE/ PIGME techniques versus neutron activation analysis (NAA) for (a) manganese and (b) chlorine for all 100 filters during 1992.

**Figure 4.21.** The PIXE/ PIGME techniques versus neutron activation analysis (NAA) for (a) bromine and (b) vanadium for all 100 filters during 1992.

**Figure 4.22.** The PIXE/ PIGME techniques versus neutron activation analysis (NAA) for (a) sodium and (b) potassium for all 100 filters during 1992.

**Figure 5.1.** The chemical database showing linkage to the meteorological database.

**Figure 5.2.** Daily values of mass, hydrogen, carbon and potassium at Wilton, July-December 1992.

**Figure 5.3.** Correlation of bromine with lead at Rozelle during the period January-June 1992.

**Figure 5.4.** Chlorine versus sodium for Cape Grim site (ASP25) for July to December 1992.

**Figure 5.5.** Average mass of fine particles in the air at all 25 ERDC sites on 6th May, 1992, a high-pollution day (Pollution Index = 54). The USA EPA goal is  $25 \text{ } \mu\text{g/m}^3$  for PM10 sulphate for 24 hours.

**Figure 5.6.** Monthly average values of lead in the air at ERDC sites for the period January-December 1992.

**Figure 5.7.** Average distribution of fine lead over the study area during July 1992.

## LIST OF FIGURES

**Figure 5.8.** Pie charts for the average percentage fine aerosol composition for (a) Rozelle an inner Sydney site, (b) Mayfield in Newcastle, (c) Warrawong in Wollongong and (d) Crookwell a rural site.

**Figure 5.9.** Average monthly mass concentrations of fine particles collected in the sectors defined in Table 5.6.

**Figure 5.10.** Distribution of total mass (PM<sub>2.5</sub>) over the ERDC study area during June 1992 (a) and December 1992 (b).

**Figure 5.11.** Monthly variations in the (TSP/PM<sub>2.5</sub>) ratio for (a) total mass, (b) iron and (c) lead at Mayfield in Newcastle.

**Figure 5.12.** Monthly variations in the (TSP/PM<sub>2.5</sub>) ratio for (a) total mass and (b) lead at Rozelle in Sydney.

**Figure 5.13.** Correlation plots of 'Soil' against its components for particles collected at Oberon during the period January-June 1992.

**Figure 5.14.** Correlation plots of 'Soil' against silicon for particles collected at all sites (a) and at Mayfield (b) during the period January-June 1992.

**Figure 5.15.** Average monthly concentrations of sulphur in fine particles collected in the sectors defined in Table 5.6.

**Figure 5.16.** Distribution of sulphur in fine particles collected over the study area during the months of June and December 1992.

**Figure 5.17.** Average sulphur concentrations on 27th December 1992 at all sites of the ERDC network.

**Figure 5.18.** Average daily lead concentrations during 1992 at (a) Mascot and (b) Oberon. The Mascot site commenced 26/2/92. At the Oberon site, values less than the minimum detectable limit (10 ng m<sup>-3</sup>) are indicated by a dotted line.

## LIST OF FIGURES

**Figure 5.19.** Annual mean and maximum lead concentrations for 1992 in the sectors defined in Table 5.6. The dotted line indicates the mean value for all sites.

**Figure 5.20.** Monthly average lead concentrations during 1992 for sectors defined by distance from Sydney (a) and for urban sectors (b). Sectors are defined in Table 5.6.

**Figure 5.21.** Lead levels at each of the sampling sites on 14 June, 1992.

**Figure 5.22.** Comparison of lead concentrations in fine particles ( $<2.5 \mu\text{m}$ ) and total suspended particulates (TSP) at (a) Rozelle and (b) Mayfield. In (a), average monthly lead in TSP (lower lines) and the maximum monthly lead in TSP (upper lines) are indicated (data from NSW EPA, 1993). In (b), lines represent average monthly lead in TSP (data from BHP Newcastle, 1993).

**Figure 5.23.** Concentrations recorded at Lidcombe during 1992 for (a) lead, (b) bromine, (c) lead/bromine mass ratio, (d) non-seawater sulphate, (e) divalent metal ions, (f) trivalent metal ions, (g) potassium, (h) ozone (data from NSW EPA, 1993), and (i) nitrogen oxides (data from NSW EPA, 1993). The dotted line in (c) indicates the lead/bromine ratio calculated on the basis of petrol composition. Non-seawater sulphate (NSS) was calculated from measured sulphur and sodium concentrations by  $\text{NSS} = 3 \cdot (\text{S} - 0.0837 \cdot \text{Na})$ .

**Figure 5.24.** Correlation of monthly-average concentrations of cobalt with iron at (a) Mayfield and (b) Warrawong, from January 1992 to July 1993.

**Figure 5.25.** Correlation of vanadium with elemental carbon at Warrawong, monthly means 1992-3.

**Figure 5.26.** Correlation of monthly-average concentrations of iron with sulphur at (a) Mayfield and (b) Warrawong and (c) Muswellbrook, from January 1992 to June 1993.

**Figure A.1.** Normalised particle scattering coefficient versus wavelength of scattered light. Adapted from Mie scattering theory (Kerker 1969).

**Figure A.2.** Particle absorption ( $b_{\text{ap}}$ ) and scattering coefficients ( $b_{\text{sp}}$ ) versus particle diameter. Taken from Waggoner et al 1981).

LIST OF FIGURES

**Figure A.3.** Respiratory deposition fractions for various human body parts as a function of particle size. Taken from the work of US Department of Health 1969.

**Figure A.4.** Retention of particle matter in the human lung in relation to particle size. Taken from Goldberg 1973.

**Figure A.5.** Plot of the mean daily mortality (from all causes) versus mean PM10 levels for 5 day lagged moving averages in Utah County, after Pope et al 1992.

## GLOSSARY

Symbol	Description
'Ammonium Sulphate'	In quotes, is an estimate of the ammonium sulphate component of the fine (PM <sub>2.5</sub> ) aerosol. Defined in Table 4.6.
ANSTO	Australian Nuclear Science and Technology Organisation
ASP	Aerosol Sampling Program
$b_0$	Absorption coefficient for particles( $\mu\text{m}^{-1}$ ) with no layering correction. Defined in equ. (4.1).
$b_{ap}$	Absorption coefficient for particles( $\mu\text{m}^{-1}$ ) with layering correction. Defined in equ.(4.2).
$b_{ag}$	Absorption coefficient for gases( $\mu\text{m}^{-1}$ ). Defined in equ.(A.2).
$b_{ext}$	Coefficient of extinction ( $\mu\text{m}^{-1}$ ). Defined in equ.(A.2)
$b_{sw}$	Scattering coefficient for water ( $\mu\text{m}^{-1}$ ). Defined in equ.(A.2)
$b_{sg}$	Scattering coefficient for gases ( $\mu\text{m}^{-1}$ ). Defined in equ.(A.2)
$b_{sp}$	Scattering coefficient for particles ( $\mu\text{m}^{-1}$ ) Defined in equ.(A.2)
Coarse particles	Particles with diameters greater than 2.5 $\mu\text{m}$
$\varepsilon$	Absorption efficiency( $\text{m}^2/\text{g}$ ) defined in equ. (4.4)
Elt.C	Elemental carbon or soot. Defined by equ.(4.4)
EPA	Environment Protection Authority
ERDC	Energy Research and Development Corporation
Fine particles	Particles with diameters less than 2.5 $\mu\text{m}$
FPM	Fine particle (PM <sub>2.5</sub> ) mass
IAEA	International Atomic Energy Agency
IBA	Ion beam analysis
IC	Ion chromatography
IMPROVE	Interagency Monitoring of Protected Visual Environments
LIPM	Laser integrated plate methods

## GLOSSARY

MAQS	Metropolitan Air Quality Study
MDL	Minimum detectable limit
NAA	Neutron activation analysis
ng	nanogram ( $10^{-9}$ gram)
NH&MRC	National Health and Medical Research Council
NHSO4	See 'Ammonium sulphate'
NOX	Oxides of nitrogen
OMH	'Organic matter' estimated from hydrogen mass. Defined in equ.(4.8)
'Organic matter'	In quotes, is an estimate of the organic matter component of the fine (PM2.5) aerosol. Defined in equ. (4.8)
PESA	Particle elastic scattering
PIGME	Particle induced gamma ray emission
PIXE	Particle induced X-ray emission
PM2.5	Particles with diameters less than 2.5 $\mu\text{m}$
PM10	Particles with diameters less than 10 $\mu\text{m}$
Q	Flow rate through the samplers (L/min). Define in eqs.(3.1 and 3.2)
R	Layering correction defined in equ.(4.3)
RBS	Rutherford backscattering
RCM	Reconstructed mass, defined in equ. (4.9)
'Salt'	In quotes, is an estimate of the sodium chloride component of the fine (PM2.5) aerosol. Defined in equ. (4.5)
SCBD	Sydney Central Business District
'Smoke'	In quotes, is an estimate of the smoke component of the fine (PM2.5) aerosol. Defined in equ. (4.7)
'Soil'	In quotes, is an estimate of the soil and ash component of the fine (PM2.5) aerosol. Define in equ. (4.6)
soot	Same as elemental carbon
SOX	Oxides of sulphur
SPCC	State Pollution Control Commission

## GLOSSARY

T	Absolute temperature (K)
$T_0$	Absolute calibration temperature in (K)
TSP	Total suspended particulates (PM50)
$\mu\text{C}$	MicroCoulombs of ion beam charge, used for analysis
$\mu\text{g}$	microgram ( $10^{-6}$ gram)
$\mu\text{m}$	Micrometer ( $10^{-6}$ m)
UCD	University of California Davis
$V_m$	Meteorological visual range. Defined in equ.(A.1)

## **1. INTRODUCTION**

This is the final report to the Energy Research and Development Corporation (ERDC) on project number 1516. This project was titled "Contributions of Fuel Combustion to Pollution by Airborne Particles in Urban and non-Urban Environments" and was funded by ERDC to the total value of \$394,556 over 3 years from the 1 January 1991 to 30 December 1993. The project management team set up and operated a large area fine particle aerosol sampling network covering 60,000 square kilometres of New South Wales. This network known as the ERDC project network consisted of 24 cyclone sampling units comprising an area extending from south of Wollongong, to north of Newcastle and west of the Blue Mountains and 1 unit at Cape Grim in north west Tasmania to provide background baseline sampling data. The majority of these fine particle sampling sites have operated since the 1 January 1992. The 3 initial pilot units established at Lucas Heights, Pyrmont and Rozelle commenced operation on 1 July 1991.

The aim of this final report is to publish some of the key data obtained and findings made by this study between 1 January 1992 and 30 June 1993. This time span includes one complete summer and winter period and two partial summer and winter periods. The report is divided up into several sections; section 1 is the introduction and discusses some of the history of the Aerosol Sampling Program (ASP), together with the ERDC project objectives; section 2 looks at the sources and characteristics of fine particles; section 3 describes the ERDC network and the units used to sample fine particles; section 4 discusses the techniques used to analyse the filters obtained during the project, and includes quality assurance aspects of the program including analysis errors and some analytical comparisons with other measurement techniques. Section 5 presents some of the results and data interpretations while sections 6 and 7 contain the project conclusions and recommendations.

### **1.1 HISTORY OF ASP**

The aerosol sampling program ASP at the Australian Nuclear Science and Technology Organisation (ANSTO) existed some time before the funding for this ERDC project became available. In the middle of 1989 the Applications of Nuclear Physics (ANP) Program Area at ANSTO established contact with the then NSW State Pollution Control Commission (SPCC), now the Environment Protection Authority (EPA), for discussions on how best to apply accelerator based ion beam analysis (IBA) techniques to aerosol pollution problems in NSW.

## SECTION 1 - INTRODUCTION

ANSTO was aware that these IBA techniques, particularly proton induced X-ray emission (PIXE), have been available to countries throughout Europe and the United States since the late 1970's and early 1980's. These techniques have been applied to the multi-elemental analysis of thousands of filter papers a year obtained from large area aerosol monitoring networks in the USA (Cahill 1990). They were carried out in the main by nuclear physics laboratories using small to medium size particle accelerators similar to the 3 MV Van de Graaff accelerator at ANSTO at Lucas Heights near Sydney. These techniques allow analysis of each filter paper for the following elements, H, C, N, O, F, Na, Al, Si, P, S, Cl, K, Ca, V, Ti, Mn, Fe, Cr, Ni, Cu, Zn, Br, and Pb. In addition filters can be analysed for soot or elemental carbon using laser techniques (Cahill 1992 and Cohen 1992). Hence it is possible to evaluate the urban and non-urban and natural and anthropogenic elemental composition of these fine aerosols.

In October 1989 officers at ANSTO put together a team of interested parties from the NSW SPCC (now the EPA), the Electricity Commission of NSW (now Pacific Power) and the School of Earth Sciences at Macquarie University to help promote these techniques and ideas in aerosol pollution research in Australia. Two key international laboratories using IBA techniques in pollution studies and aerosol analysis at the time were the University of Lund in Sweden and the University of California, Davis (UCD). This team applied for support from the Australian Department of Industry, Trade and Commerce (DITAC) for a workshop to be held at the UCD on Ion Beam Techniques in Pollution Studies. The application for Workshop support with DITAC was successful and the workshop at UCD took place in September 1990. Four members from the team represented Australia at this Workshop. They were able to see first hand the fine aerosol sampling units used in the IMPROVE network and to obtain copies of their sampling protocols and have detailed discussions regarding data analysis and interpretation. In addition 25 cyclones were supplied at cost to ANSTO by the UCD Workshop for this study.

Early in 1990 a consortium, consisting of the NSW EPA, Pacific Power, University of NSW (School of Chemical Engineering and Industrial Chemistry), and ANSTO, was formed and applied to the Energy Research and Development Corporation (ERDC) for funding, \$400,000 over 3 years, to establish a large area fine particle monitoring network in NSW. The estimated total project costs in 1990 were around \$1.2M including nearly 12 man-years of effort for the 3 year study. The extra funds, above that provided by ERDC, were in-kind contributions, access to facilities and effort supplied by the consortium members.

## SECTION 1 - INTRODUCTION

A management committee, chaired by the Pacific Power representative and with the NSW EPA representative as secretary, was established in January 1991 to run the ERDC project. The committee consisted of at least one representative from each of the major contributing organisations, namely, the NSW EPA, Pacific Power, the University of NSW and ANSTO. Dr Robert Hyde from Macquarie University was invited to join the management committee to assist in meteorological aspects of the project. In all over 36 meetings were convened during the life of the project. The principal investigator for the ERDC project was the ANSTO representative and ANSTO was the guarantor organisation for the project.

### 1.2 PROJECT OBJECTIVES

The objectives of this ERDC funded study were:

- (a) To establish a fine particle monitoring network covering the greater Wollongong/ Sydney/ Newcastle areas;
- (b) To investigate the relationships between fuel combustion and fine particle aerosols in urban and non-urban environments;
- (c) To create a database of baseline information on concentrations of fine particles resulting from such processes as fossil fuel burning and industrial manufacturing;
- (d) To identify and quantify sources of fine particles in New South Wales;
- (e) To introduce into Australia accelerator based Ion Beam Analysis (IBA) techniques for the analysis of filter papers obtained from large scale monitoring networks.

### 1.3 THE SCOPE OF THE ERDC STUDY

The initial proposal called for the design, construction and placement of 20 fine particle aerosol sampling units across the Illawarra, Sydney and Lower Hunter area and to operate these for 12 months from the 1 July 1992 to 30 June 1993. During this time it was expected that the project would collect more than 2500 Teflon filters from the network and that each of these would be analysed for more than 20 different key

elements using the accelerator based ion beam analysis techniques at ANSTO. Furthermore, other more commonly used techniques, such as, ion chromatography (IC) for cations, laser integrated plated methods (LIPM) for elemental carbon (Lin et al 1973) and neutron activation analysis (NNA) would be performed on these filters to expand the dataset and for quality assurance and control.

With the funds made available through ERDC and the support of the consortium members the project was able to place 25 sampling units (rather than the 20 originally envisaged) and to run these for 18 months from, 1 January 1992 to 30 June 1993.

#### **1.4 PREVIOUS PARTICLE STUDIES IN THE ERDC PROJECT AREA**

A number of intensive air quality studies were carried out in Sydney in the late 1970's and early 1980's. The objective of these studies was to provide background information about the conditions and interactions of the physical and chemical properties of Sydney's atmosphere. A number of universities, government departments and research organisations collected aerosol, meteorological, source emission (mobile and stationary), and visibility data over a range of time periods. In 1982 a conference was held at Leura to disseminate the results of these investigations (Carras and Johnson, 1983).

Williams et al (1983) determined the correlation between the measured light scatter and total suspended particle. Motor vehicles were found to be a major source of haze, with diesel engine vehicles (then 5% of the urban vehicle fleet), considered responsible for about half the particle emissions.

Roberts et al (1983) presented average composition of total suspended particles from sites within the Parramatta River Valley and the inner metropolitan areas but were unsuccessful in obtaining samples for haze aerosol analyses (particles < 2.5  $\mu\text{m}$  aerodynamic diameter). Their efforts however indicated that anthropogenic species such as lead, zinc, copper, bromine and sulphur occurred in particles < 10  $\mu\text{m}$  in diameter (PM10). Analyses for inorganic ions such as sulphate, nitrate, chloride and bromide were also carried out. They further reported that total carbon accounted for 30% of the average composition of Sydney brown haze.

Milne et al (1983) in a similar study concluded that one third of the winter haze was due to emissions from incineration sources, one third from motor vehicle emissions and one

## SECTION 1 - INTRODUCTION

third from other sources. Further investigation (Milne et al 1984) has established that petrol-powered and diesel-powered vehicles contribute about equally to that fraction of the brown haze attributed to motor vehicles. About 86% of the particle matter from this diesel exhaust was less than 1  $\mu\text{m}$  in diameter (Williams et al 1989).

Williams et al (1983) reported the results of an aircraft measurement program which measured the extent and distribution of Sydney brown haze across the Sydney urban region. Atmospheric samples were analysed for sulphur dioxide and the haze intensity determined from the results of a fast (5 second) nephelometer mounted in an aircraft. Major sources of sulphur were found at the Botany Bay and Silverwater petrochemical complexes. Williams observed that the haze was widespread indicating a multiplicity of sources and that there were significant sources of haze in the western areas of the Sydney region.

A report on the Koorangang and Inner Newcastle Airshed Study (KINAS) was completed by Bridgman et al (1992), Bridgman and Whitelock (1993) and Manins (1993). These papers reported on the emissions inventory and modelling of  $\text{SO}_2$ ,  $\text{NO}_x$  and total suspended particulates (TSP) for the industrial and surrounding areas of inner Newcastle for the year 1990. They found particle emissions to be typically twice the  $\text{SO}_2$  and  $\text{NO}_x$  emissions and that the NSW EPA goals for TSP were regularly exceeded. Manins (1993) concluded that stack, surface and fugitive emissions are poorly understood and not well characterised with respect to size and composition.

## 2. SOURCES AND CHARACTERISTICS OF AEROSOLS

To understand particle source apportionment, the chemical and physical characteristics of ambient particles, their variations in space and time and the relationship of these to size distributions must be studied. The impact of particles on the atmospheric environment depends in a direct way on the particle lifetimes, sizes and abundances. The work of Jaenicke (1980) shows that particles with diameters less than  $0.001\ \mu\text{m}$  and greater than  $100\ \mu\text{m}$  reside for only a few minutes in atmosphere. While particles in the  $0.1\ \mu\text{m}$  to  $1\ \mu\text{m}$  in diameter range may have residence times of several weeks in the troposphere. The action of volcanoes, for instance, may inject these fine particles into the stratosphere (Morales et al 1993) where residence times can be measured in years and the effects can be global.

Typical atmospheric particles can range in size from  $0.001$  to  $100\ \mu\text{m}$  and have concentrations ranging from a few nanograms per cubic metre of air to a few kilograms per cubic metre of air (for example: in stacks and industrial situations). Atmospheric aerosols in the size range  $0.01$  to  $10\ \mu\text{m}$  are studied for five main reasons, namely:-

- (a) They are small enough to penetrate deep into the human lung system and can be absorbed directly into the blood stream. This may have significant health related effects.
- (b) They are fine enough to remain in the atmosphere for sufficient time to be transported long distances.
- (c) They impair visibility by both light scattering and light absorption. Visibility is a key parameter that affects the public's perception of how bad a pollution problem may be. The USA fine particle IMPROVE monitoring network operates in national parks throughout North America to provide information on light scattering particles.
- (d) Aerosols affect climate and weather. Sulphate particles are important for cloud nucleation, affect the earth's albedo and therefore the tropospheric cooling (Charlson et al, 1990). Elemental carbon absorbs and scatters solar radiation affecting the earth's radiation balance (Shaw, 1982). This has been observed in Arctic areas each spring as "Arctic Haze" produced by long range transport

of anthropogenic combustion particles (Rahn & McCaffrey, 1980). Naturally occurring events such as volcanic eruptions and major fires also provide information on the global temperature effects of fine particles (Hansen et al, 1980 and Morales et al 1993).

- (e) Particle matter also deposits on vegetation and buildings, affecting their health and/or longevity.

More details concerning visual impairment, and the health and climate effects of aerosol particles are given in Appendix A.

## 2.1 SOURCES OF AIRBORNE PARTICLES

Sources of atmospheric particles are both anthropogenic and natural and in 1984 were estimated globally to be in excess of  $1.5 \times 10^9$  tonnes/ year (Prospero 1984). Currie 1992 states that global natural sources exceed global anthropogenic sources by about a factor of five, although each component is uncertain by at least a factor of two. Anthropogenic sources tend to be concentrated in heavily populated areas, so although their global concentrations may be smaller than those of natural sources their effects can be more significant.

Global anthropogenic emissions are dominated by sulphates (71%) with nitrates a distant second (13%), while natural emissions are dominated by sulphates (27%), sea salt (40%) and windblown dust (20%) (Prospero 1984). Sources of anthropogenic particles in the atmosphere include motor vehicles, power generation, industrial, combustion processes, mining and quarrying and agricultural processes. Recent source emission work in Australia (Carnovale et al, 1992) showed that, for anthropogenic PM10 particles on a typical summer day in Melbourne in 1990, 45% was attributed to motor vehicles, 30% to industrial/commercial point sources such as metals manufacture and petrol refining, and 25% to sources such as waste combustion and lawn mowing. Comparable data for Sydney is currently being collected as part of MAQS. Sources of natural particles include ocean seaspray, windblown dust, volcanoes and forest fires.

Particle emissions from anthropogenic and natural sources, can be associated with groups of elements, for example: particles from motor vehicles with Pb, Br and Cl, seaspray with Na and Cl and coal burning, metal smelting and some natural sources with sulphur. (Table 2.1)

SECTION 2 - SOURCES AND CHARACTERISTICS OF AEROSOLS

**Table 2.1(a)** Fuels, their uses and elements commonly found in particles resulting from their combustion.

<b>Fuel Type</b>	<b>Uses</b>	<b>Element</b>
<b>Coal</b>	Power generation Smelting metals Process heating	C, N, O, H, S, Si, Al, Ca, Fe, Se, Ba, V, Ni, F, Na, As
<b>Petroleum</b>		
Fuel Oil:	Power generation Process heating Space heating	C, H, O, S, V, Ni
Diesel:	Transport Agriculture	C, H, O, N
Petrol:	Motor vehicles Aviation	C, H, Pb, Br, Cl, S
Gas:	Motor vehicles Process heating Domestic heating	C, H, O, N
<b>Wood</b>	Domestic heating Controlled burning	C, H, O, K, Zn, Ca, Cl
<b>Wastes</b>	Industrial Municipal Domestic	C, Na, K, Cl, Ca, Zn, Pb, Sb, Se, Cd

**Table 2.1(b)** Industrial processes, their uses and elements commonly associated with them.

Process	Element
Steel-Making	Fe, Mn, Ca, Ni, Mo
Copper Smelting	Cu, Fe, Zn, Pb, S, As, Cd
Aluminium Smelting	Al, F, Si, Na, C
Petrol Refining	C, H, V, Ni
Cement Making	Ca, Si, Al, C, O
Fertiliser Manufacture	Cr, P, F, Si, S, O

**Table 2.1(c)** Natural particles. and elements commonly associated with them.

Class	Element
Seasalt	Na, Cl, Mg, S, Ca, K
Soil	Si, Al, Ca, Mg, Ti, V, Fe, K, Mn, Sr, Zr, Na, C, N, P, H, O
Terpene Oxidation Products	C, H, O
Pollen, Spores, Bacteria, Viruses	C, H, O, K, Na, Ca

## 2.2 CHARACTERISTICS OF AIRBORNE PARTICLES

There are several processes that affect the removal rate of particles from the atmosphere. These include diffusion and impaction for smaller particles ( $< 1 \mu\text{m}$ ), settling and sedimentation for larger particles ( $> 1 \mu\text{m}$ ) and wet deposition. The removal rate for small particles decreases as size increases, while for larger particles it decreases as size decreases. Figure 2.1 shows the dry removal rate of particles with diameters between  $0.01 \mu\text{m}$  and  $100 \mu\text{m}$ .

## SECTION 2 - SOURCES AND CHARACTERISTICS OF AEROSOLS

Measurements of the mass of aerosols collected on a filter would show a bimodal distribution in particle diameter with a peak in the fine particle mass at around 0.1 to 1  $\mu\text{m}$ . This peak corresponds to the decrease in the removal rate shown in Figure 2.1. Figure 2.2 shows schematically this bimodal particle mass distribution as a function of particle diameter. There is a natural minimum at around 2.5  $\mu\text{m}$  particle diameter. Above this diameter, although the removal rate increases, the total particle mass continues to increase. In fact, for a given particle density the mass increases as the cube of the diameter and this causes the curve to increase up to and beyond 10  $\mu\text{m}$  diameters. However, at some point the removal rate for very large particles is sufficiently large to turn this curve over again and the contribution to the total mass from particles > 50  $\mu\text{m}$  in diameter is usually small and decreases above this diameter.

The naturally occurring minimum in the mass versus size distribution at 2.5  $\mu\text{m}$  diameter defines two modes of formation, commonly referred to as the accumulation mode (< 2.5  $\mu\text{m}$ ) and the mechanical mode (> 2.5  $\mu\text{m}$ ). The accumulation mode particles are typically produced by combustion processes such as fossil fuel burning, bush fires and industrial combustion. Fine particles in this mode contain sulphates, nitrates, elemental carbon, organic compounds and lead. Coarse particles in the mechanical mode are typically produced by grinding, crushing or windblown processes and contain particles such as mineral dust, soils, sea salt, pollens, plant spores, coarse particles from industry and coagulated fine particles.

Table 2.2 shows the size range of some common sources of fine and coarse particles. Some typical sizes for the diameter of human hair and sizes for which human lung damage and significant light scattering may occur are shown for comparison purposes. As the limit of visibility of the human eye is generally considered to be around 50  $\mu\text{m}$  most of these particles are visible.

Figure 2.2 shows clearly the desirability of using 2.5  $\mu\text{m}$  diameter or less (PM<sub>2.5</sub>) as a natural particle size cut off for monitoring fine atmospheric aerosols. The PM<sub>10</sub> or 10  $\mu\text{m}$  diameter or less cut off contains the accumulation mode (< 2.5  $\mu\text{m}$ ) as well as contributions from the mechanical mode. Therefore, to study particles in the accumulation mode alone it is preferable to use a sampling unit with a PM<sub>2.5</sub> cut off.

**Table 2.2** Particle size ranges for a series of commonly occurring aerosols

Type	Size ( $\mu\text{m}$ )
Smog	0.01 - 2
Oil Smokes	0.03 - 1
Tobacco Smokes	0.01 - 1
Carbon Black	0.01 - 3
Zinc Oxide Fume	0.01 - 3
Plant Spores	10 - 30
Bacteria	0.3 - 30
Clouds and Fog	2 - 60
Coal Dust	1 - 100
Cement Dust	3 - 100
Human Hair	30 - 200
Lung Damage	0.5 - 5
Light Scattering	0.5 - 5
Visible to Eye	50 upwards

Another commonly used size selective term is the total suspended particulate matter or TSP. This refers to all particle sizes collected on a filter by a standard high volume sampler and usually includes all particles with diameters less than about 50  $\mu\text{m}$ . This size regime includes both the accumulation mode and the mechanical mode but is generally dominated by the mechanical mode mass with the fine particle mode contributing a few tens of percent to the total mass. It is therefore very important both to understand the differences between these size modes and to measure the particle size distribution to fully understand the mechanisms producing these particles. The relative contribution of the fine and coarse modes shown in Figure 2.2 can also differ significantly with time or season and with site.

The bimodal distribution of mass versus particle diameter is illustrated by measurements plotted in Figure 2.3. Measurements from a manganese smelter show a particle size distribution with a peak in the fine mode at around 0.7  $\mu\text{m}$  diameter and a second peak in the

coarse mode at 7  $\mu\text{m}$ , reflecting both combustion and mechanical components in the process. Integrating the areas under the curve shows 74% of particles occur in the fine mode and 26% in the coarse mode. Data from the plume of a coal fired power station in Tennessee, USA ( Kim et al 1989), shows presence of particles in the fine mode, with the peak occurring between 0.1 and 1  $\mu\text{m}$  diameter. The coarse mode particles from this combustion process were removed by the venting the plume through a 99.5+% efficient electrostatic precipitator.

These examples clearly demonstrate the importance of knowing the particle size distribution. For instance, both the power station and the smelter may have the same total suspended particulate (TSP) levels, however, for the manganese smelter the aerosol mass associated with coarse mode ( $> 3 \mu\text{m}$ ) is nearly 300 times more than the mass associated with the fine mode ( $< 3 \mu\text{m}$ ). The mass on the TSP filter would be dominated by the properties associated with the coarse mode, in spite of the fact that there were nearly 3 times as many fine particles as coarse particles present.

### 2.3 POLLUTION GUIDELINES OR GOALS

Comprehensive air quality goals for urban air pollutants have not been defined in New South Wales at the present time. The NSW EPA states that "there are insufficient Australian data on health effects of these pollutants to allow their adequate determination". Consequently, the NSW EPA refers to the National Health and Medical Research Council (NHMRC) guidelines, World Health Organisation long term goals and US EPA air quality standards for our local NSW goals.

In the United States there are two sets of ambient air quality standards, those for the State of California and those for the rest of the United States. These two standards are reproduced in Table 2.3 for a range of particle and gaseous air pollutants. The Californian standards are generally similar or lower than the equivalent national US standard.

Some of these standards have been noted by New South Wales EPA as goals and are shown in Table 2.4. There are no goals for fine (PM<sub>2.5</sub>) particles. Of the 25 different elemental components measured by the ERDC network, there are goals set for sulphate (25  $\mu\text{g}/\text{m}^3$  in 24 hr) and lead (1.5  $\mu\text{g}/\text{m}^3$  over 90 days). Both these goals relate to the TSP mode not the fine mode.

## SECTION 2 - SOURCES AND CHARACTERISTICS OF AEROSOLS

**Table 2.3** Ambient Air Quality Standards for California and the USA

Pollutant	Averaging Time	California Standard Concentration	National Standards Primary
Ozone	1 hour	0.09 ppm (180 $\mu\text{g}/\text{m}^3$ )	0.12 ppm (235 $\mu\text{g}/\text{m}^3$ )
Carbon Monoxide	8 hour	9.0 ppm (10 $\mu\text{g}/\text{m}^3$ )	9.0 ppm (10 $\mu\text{g}/\text{m}^3$ )
	1 hour	20 ppm (23 $\mu\text{g}/\text{m}^3$ )	35 ppm (40 $\mu\text{g}/\text{m}^3$ )
Nitrogen Dioxide	Annual Average	-	0.053 ppm (100 $\mu\text{g}/\text{m}^3$ )
	1 hour	0.25 ppm (470 $\mu\text{g}/\text{m}^3$ )	-
Sulphur Dioxide	Annual Average	-	80 $\mu\text{g}/\text{m}^3$ (0.03 ppm)
	24 hour	0.05 ppm (131 $\mu\text{g}/\text{m}^3$ )	365 $\mu\text{g}/\text{m}^3$ (0.14 ppm)
	1 hour	0.25 ppm (655 $\mu\text{g}/\text{m}^3$ )	-
Suspended Particulate Matter (PM10)	Annual Geometric Mean	30 $\mu\text{g}/\text{m}^3$	-
	24 hour Annual Arithmetic Mean	50 $\mu\text{g}/\text{m}^3$ -	150 $\mu\text{g}/\text{m}^3$ 50 $\mu\text{g}/\text{m}^3$
Sulphates	24 hour	25 $\mu\text{g}/\text{m}^3$	-
Lead	30 Day Average Calendar Quarter	1.5 $\mu\text{g}/\text{m}^3$ -	- 1.5 $\mu\text{g}/\text{m}^3$
Hydrogen Sulphide	1 hour	0.03 ppm (42 $\mu\text{g}/\text{m}^3$ )	-
Vinyl Chloride (chloroethene)	24 hour	0.010 ppm (26 $\mu\text{g}/\text{m}^3$ )	-

SECTION 2 - SOURCES AND CHARACTERISTICS OF AEROSOLS

**Table 2.4** Ambient air quality goals for New South Wales as adopted from various US EPA and NHMRC goals.

Pollutant	Standard	Agency
<b>Particles</b>		
TSP (annual av.)	90 $\mu\text{g}/\text{m}^3$	NHMRC
PM10 (annual mean)	50 $\mu\text{g}/\text{m}^3$	USEPA
PM10 (24hr max.)	150 $\mu\text{g}/\text{m}^3$	USEPA
Lead TSP (90 day av.)	1.5 $\mu\text{g}/\text{m}^3$	NHMRC
<b>Gases*</b>		
Ozone (1hr max.)	235 $\mu\text{g}/\text{m}^3$ (0.12 ppm)	NHMRC
NO <sub>2</sub> (1hr max.)	300 $\mu\text{g}/\text{m}^3$ (0.16 ppm)	NHMRC
SO <sub>2</sub> (1hr max.)	655 $\mu\text{g}/\text{m}^3$ (0.25 ppm)	NHMRC
CO (8hr max.)	10 $\mu\text{g}/\text{m}^3$ (9 ppm)	NHMRC

\* conversions to  $\mu\text{g}/\text{m}^3$  using 25°C and 1 atmosphere

### 3. THE AEROSOL SAMPLING NETWORK

The study area covers 60,000 square kilometres of NSW, stretching 300km along the coast, from north of Newcastle to south of Wollongong and up to 200km inland, to Mudgee in the north and Crookwell in the south (Figure 3.1). The area includes the major population areas of NSW, the major industrial sites of Wollongong and Newcastle, and covers the three electricity generating regions comprising seven coal fired power stations. The cities of Newcastle and Wollongong are major industrial centres with industries such as iron and aluminium smelting, sulphuric acid plants, lead and zinc production and fertiliser works.

#### 3.1 SITE LOCATIONS

The locations of the 24 ERDC sites are shown in Figure 3.1; the 25th site is located at the global baseline station at Cape Grim in north west Tasmania. The 24 sites include, at one extreme, highly urbanised and industrialised locations and at the other, rural sites adjoining large areas of national parks and virgin bushland.

The network was designed to monitor particles in a range of different environments and from a range of processes. These included power generation (Muswellbrook - ASP 4; Cullen Bullen - ASP 22; Doyalson - ASP 24) and industrial processes (Warrawong - ASP 8; Mayfield - ASP10). Other sites such as Badgery's Creek (ASP 21), Mascot (ASP23) and Richmond (ASP18) and Campbelltown (ASP6) were chosen because of their positions in the Hawkesbury and Sydney basins and the increasing public concern about pollution in these areas. Inner city sites such as Pyrmont (ASP2) and Rozelle (ASP3) were chosen for comparison with out-lying rural sites like Oberon (ASP13) and Crookwell (ASP20) and to provide data on fine particles from motor vehicles (expected to be a major source of fine particles in the inner city region).

The location, starting date, site number and an approximate classification for each of the 25 ERDC sites are given in Table 3.1.

SECTION 3 - THE AEROSOL SAMPLING NETWORK

**Table 3.1.** Approximate classification of the sampling sites for the ERDC project. Definitions of site type depends upon the weighting given to different environmental land use factors.

Type	Location	Starting Date	Site no.
Natural	Cape Grim	22/6/92	25
Rural	Putty	3/2/92	16
	Oberon	18/12/91	13
	Crookwell	6/2/92	20
	Mudgee	23/1/92	15
	Wilton	8/1/92	14
Rural urban	Badgerys Creek	7/2/92	21
	Moss Vale	14/2/92	19
	Richmond	20/2/92	18
Rural industrial	Muswellbrook	29/9/91	4
	Cullen Bullen	13/2/92	22
	Doyalson	26/2/92	24
	Tomago	8/12/91	11
	Campbelltown	30/10/91	6
Urban non- industrial	Blackheath	18/12/91	12
	Albion Park	30/10/91	7
	Lucas Heights	3/7/91	1
	Macquarie University	31/1/92	17
Urban industrial	Bellambi	13/11/91	9
	Rozelle	18/7/91	3
	Pymont	4/7/91	2
	Lidcombe	2/10/91	5
Urban heavy industrial	Mayfield	8/12/91	10
	Warrawong	25/12/91	8
	Mascot	25/2/92	23

## 3.2 DESCRIPTION OF SAMPLING OPERATIONS

### 3.2.1 The Sampling Unit

The sampler unit used throughout the ERDC project was based on Module A of a four filter module system used across the USA by the IMPROVE network (Eldred et al 1988). Module A uses a 25 mm diameter stretched Teflon filter with 99.79% aerosol retention for 3µm diameter particles and provides the bulk of the fine aerosol information for the IMPROVE network.

A photograph of the ERDC sampler unit designed and built at ANSTO is shown in Figure 3.2 and a schematic diagram of the panel layout in Figure 3.3. The unit is contained in a weather proof enclosure and generally mounted on two 2m high posts. Each unit has a sun shield attached to the top and back and was sited with the rear of the unit facing north. The Thompson diaphragm pump was situated on a raised plinth at the base of the unit in its own pump housing (see Figure 3.4). The schematic diagram of Figure 3.5 shows the air flow through the system. Air is drawn in through the stack into the cyclone where particles of 2.5µm diameter and less are selected. Air is then drawn through the Teflon filters placed on top of the cyclone, into a manifold containing an adjustable orifice and then out through the vacuum pump.

### 3.2.1 The Filter

The Teflon filters were transported to the site before exposure and from the site to Lucas Heights after exposure in their cassettes. They were not handled at any stage by the field operators. Each unit contained a seven day programmable clock to turn the pump on at any time. The unit at each site was operated on Wednesday and Sunday for 24 hours from midnight to midnight. The filters were changed once a week usually on a Monday or Tuesday, since each sample operated on separate channels. The 2 colour coded filter cassettes containing the Teflon filters were unscrewed from the cyclone head and the manifold placed in a 'Tupperware' box with the logsheet for that week and posted to Lucas Heights for analysis. Figure 3.7 shows a 'Tupperware' box and its standard contents. Each site had its own filter cassettes and 'Tupperware' boxes to minimise cross contamination. This postage system worked extremely well for all sites over the study period, with no boxes being lost and most arriving within a week of

posting. At the end of every month the logsheets for all sites were entered into a computer file which was linked with the analysis data file for those filters. Figure 3.8 shows the collection and analysis efficiency for 1992 for all sites. The average for the year was nearly 97%, while the lowest monthly efficiency was 93% in May 1992. Many sites regularly maintained a 100% collection efficiency of filters. After each filter had been analysed using the ion beam analysis techniques it was stored in a library of filters for future reference and for analysis by other techniques such as ion chromatography.

### 3.2.3 Sampler Calibrations

In order to achieve good particle size selectivity, a constant flow rate should be maintained through the cyclone, (Figure 3.6). The flow is controlled by the critical orifice between the solenoids and the hose to the pump (Figure 3.5). The flow rate ( $Q$ ) through this orifice is dependent on the pressure drop ( $\delta P$ ) across the cyclone and the absolute temperature ( $K$ ) of the airstream, by (Eldred et al 1988),

$$Q = a (\delta P)^b (T/T_0)^{1/2} \quad (3.1)$$

where  $a$  and  $b$  are constants determined for each sampler at each site for a given temperature  $T_0$ . These constants were determined by measuring the pressure drop across the cyclone with a Magnehelic gauge for various flowrates as measured with a calibrated rotameter gauge. Figure 3.9 shows such a calibration curve for the Lucas Heights sampler (ASP1) for rotameter flow rates from 10 to 25 L/min. Typical values for the constants were  $a=4.151$ ,  $b=0.3377$  and  $T_0=293K$ . The unit was designed for a 2.5  $\mu m$  diameter cut off at  $Q=21.7$  L/min flow rate which corresponds to a Magnehelic gauge reading of  $\delta P=134$  Pa, (John and Reischl, 1980). If the Magnehelic reading after filter exposure was less than 50% of this reading (ie.  $< 72$  Pa) a warning error code (see section 4.4) was attached to this filter in the database. A 50% drop in the Magnehelic reading corresponded to about 20% drop in the flow rate  $Q$  to 17.2 L/min. Figure 3.6 shows this drop increases the cyclone diameter cut off from 2.5  $\mu m$  to about 3.1  $\mu m$ . Typically flow rates changed by less than 10% except for the most heavily loaded filters and the 2.5  $\mu m$  diameter cut off was essentially maintained.

During the year, temperatures at sites varied from less than  $0^\circ C$  at night to over  $40^\circ C$  in the middle of the day. This temperature deviation from the calibrated temperature  $T_0$

affected the flow rate. Equation 3.1 shows that a  $\pm 20^{\circ}\text{C}$  variation around an ambient temperature of  $20^{\circ}\text{C}$  ( $T_0=293\text{K}$ ) corresponds to a flow rate change of -4% to +3% from the ambient value. Hence large temperature variations were not a problem.

The network logsheets recorded the ambient maximum and minimum temperatures and the pre- and post- exposure Magnehelic reading. This allowed mean flow rates and hence the total sampled volume of air through the cyclone for each sampler at each site on each day to be calculated from a calibration curve similar to that shown in Figure 3.9. These values were linked with each filter analysis in the database and used to convert the mass concentration on the filter to mass per cubic metre equivalents of air sampled.

Each sampling unit has two pressure gauges, the Magnehelic gauge and the vacuum gauge. The vacuum gauge is used as a backup. It measures the pressure in the manifold (see Figure 3.5) and is less accurate than the Magnehelic gauge. It was calibrated against flow rate through the critical orifice and its readings logged before and after filter exposure. If the Magnehelic system failed, the backup system could be used to monitor the flow rate and hence the total volume of air sampled during one 24 hour sampling period. The pressure in the manifold system is a linear function of flow rate and was fitted to an empirical function of the form:

$$Q = (a - b \Delta P) (T/T_0)^{1/2} \quad (3.2)$$

where  $\Delta P$  is the vacuum gauge reading (kPa) and  $T$  is the absolute calibration temperature (K). The calibration curve for the ASP1 unit at Lucas Heights for the vacuum gauge readings is shown in Figure 3.10. The typical constants are  $a=27.34$ ,  $b=0.2706$  and  $T_0=293\text{K}$ . A flow rate of  $Q=21.7$  L/min for a  $2.5 \mu\text{m}$  diameter cut off corresponds to a vacuum gauge reading of 21 kPa at  $20^{\circ}\text{C}$ .

## 4. ANALYSIS TECHNIQUES

### 4.1 ION BEAM ANALYSIS (IBA) TECHNIQUES

When a light ion such as a proton or helium ion from an accelerator interacts with an atom in the target material several reaction processes are possible. Some of these processes are shown schematically in Figure 4.1. The incoming ion from an accelerator interacts with the target atom electron cloud producing ionisation (electron ejection) and subsequent photon emission, usually an X-ray photon. This photon is characteristic of the target atom struck and the process is called particle induced X-ray emission (PIXE). Inelastic interactions with the target atom nucleus may scatter the incoming ion, producing gamma rays, this is called particle induced gamma ray emission (PIGME), or interact with the nucleus producing other light particles, this is called nuclear reaction analysis (NRA). Elastic interactions with the target atom nucleus may scatter the incoming ion in a "billiard ball" type interaction. This process is called Rutherford backscattering (RBS) if the ion is scattered backwards or particle elastic scattering (PESA) if the incoming ion glances off the nucleus and is forward scattered. Furthermore, ion interactions with several target atoms may break chemical bonds, produce light or UV, sputter atoms from the surface itself or, if the target has its own crystalline structure, channel the incoming ion along the ordered rows of atoms in the target. The result of all these processes is the ion loses energy in the target material and products are produced which when detected can provide valuable information about the target's elemental composition with very high sensitivities. These processes are the essence of accelerator based ion beam analysis techniques and have been described in detail by Cahill (1992) and Cohen (1992).

Accelerator based IBA techniques are ideal for elemental analysis of aerosols. They are fast, non-destructive, require no sample preparation and can analyse submicrogram samples on a filter paper in just a few minutes of accelerator machine time for all elements simultaneously. The range of possible elements covers most of the periodic table including hydrogen with more than sufficient sensitivity. Furthermore, because the techniques are so fast hundreds of samples a day can be analysed for this wide range of elements.

The four ion beam analysis techniques used simultaneously throughout this project were:

- (a) PIXE - Particle induced x-ray emission, useful for the analysis of elements from silicon to uranium in concentrations from a few  $\text{ng/m}^3$  upwards.

## SECTION 4 - ANALYSIS TECHNIQUES

- (b) PIGME - Particle induced gamma ray emission, useful for the analysis of light elements such as Li, B, F, Na, Mg, Al and Si in concentrations above  $100 \text{ ng/m}^3$ .
- (c) PESA - Particle elastic scattering analysis, useful for the analysis of hydrogen at all levels down to  $20 \text{ ng/m}^3$ .
- (d) RBS - Rutherford backscattering, useful for the analysis of very light elements such as carbon, nitrogen and oxygen in concentrations above several hundred  $\text{ng/m}^3$ .

The particle beams used throughout the ERDC work were 2.6 MeV proton beams from the ANSTO 3 MV Van de Graaff accelerator (Cohen 1992). Typical beam currents of 10 nA over a diameter of 8 mm meant that ion beam current densities on the thin Teflon filters were always less than  $0.3 \text{ nA/mm}^2$ . Run times under these conditions were of the order of 5 minutes per filter for a full multi-elemental analysis.

In general, analytical techniques with capabilities of detecting elemental concentrations of parts per million by weight on milligram samples will have the ability to quantify nanograms of material in the sample. Aerosol filter papers are such samples, typically weighing around  $100 \text{ }\mu\text{g/cm}^2$  with elemental concentrations several orders of magnitude below this. The accelerator based ion beam analysis techniques discussed here are ideally suited to perform such elemental analyses of filters. Cahill 1990 demonstrates that IBA techniques have been used to detect elemental quantities as small as  $50 \text{ pg/m}^3$  of air obtained from only  $50 \text{ }\mu\text{g}$  of sample on a filter.

### 4.1.1 Particle Induce X-ray Emission (PIXE)

Particle induced X-ray emission or PIXE became popular as an analytical tool in nuclear physics laboratories in the mid 1970's following a review on the its applications by Johansson and Johansson (1976) from the University of Lund in Sweden. PIXE now has a world wide following with many small accelerator laboratories operating their own analytical facilities. There are currently over 100 laboratories in more than 30 different countries throughout the world operating PIXE systems. The earliest publications on PIXE included analyses of aerosol filter papers and this work still continues today (Vis 1990). The technique of using light ion beams from accelerators to induce X-rays characteristic of the target being bombarded has been reviewed over the years

(Johansson and Campbell 1988) and Cohen and Clayton (1989)) and will not be treated again in depth here.

The X-ray signals produced by ion bombardment of a target atom generate a unique fingerprint for that target atom. That is the X-ray energy or position of the peak in a spectrum determines the element present in the target and the number of X-rays in this peak specifies the amount of that element in the target. We use the PIXE technique to analyse for the 18 elements Al, Si, P, S, Cl, K, Ca, Ti, V, Cr, Mn, Fe, Co, Ni, Cu, Zn, Br and Pb simultaneously. Figure 4.2 shows typical PIXE spectra obtained for the sites at Mascot (ASP23) an inner Sydney suburb and Oberon (ASP13) a rural site on the same day, 24 June 1992. The number of peaks and hence the number of elements present in the two spectra are clearly different. Peaks corresponding to X-rays for elements from Al to Pb are readily seen. Each of these peaks not only identifies an element present in the aerosol but can also be linked to a particular source. For example, Al and Si are associated with windblown soil, S with fossil fuel burning, Cl with sea spray, K with smoke and wood burning, Cr, Mn, Fe, Cu and Zn with industrial processes and Pb and Br from motor vehicles. Hence proper analysis of spectra like those shown in Figure 4.2 can be powerful methods for source reconciliation whenever detailed source fingerprints are known. At a glance we see that there is very little industry or motor vehicle aerosol contribution at Oberon compared with Mascot, whereas both sites have contributions from windblown soil, fossil fuel burning and seaspray.

The characteristic elemental peaks of Figure 4.2 sitting on the background vary in height over several orders of magnitude. They represent elemental concentrations down to a few parts per million by weight and clearly demonstrate the power of the PIXE technique for elemental analysis over several orders of magnitude in concentration. The dashed curve corresponds to the experimental data and the solid curve is a theoretical fit produced by the computer codes generated at ANSTO (Clayton 1986). These codes enable us to find the peak areas and hence the elemental concentrations in the aerosol sample. The background underneath the peaks falls by 2 orders of magnitude between X-ray energies 2 and 5 keV, being essentially zero above 6 keV as shown in Figure 4.2. This lack of background in the X-ray region above several keV is the reason for the high sensitivity of PIXE in the Ca to Zn region of the periodic table compared to other X-ray analytical techniques such as X-ray fluorescence (XRF), see Maenhaut (1989 and 1990).

The number of X-rays for each  $\mu\text{g}/\text{cm}^2$  of material on the filter, per 3  $\mu\text{C}$  run on the accelerators for each element in the periodic table from aluminium to uranium is shown

in Figure 4.3. Two different X-ray line series, K lines and L lines, originating from the ion beam interacting with K or L shell target atom electron are used for the analysis. Typically K lines are used for elements below Zr (X-ray energies between 1 and 16 keV energy) and L lines for elements above tungsten (X-ray energies above 8 keV). Using these two series coverage of most of the period table between Al and U is possible, with yields of 100 counts per peak or more.

For these analyses 2.6 MeV proton beams were used exclusively, which means that the velocity of the ions striking the aerosol filters is about 7.4% the speed of light hence most protons pass straight through the filter with very little energy loss (< 1%). As a result, IBA methods are non-destructive and the Teflon filters can be used for further analysis by techniques such as ion chromatography or neutron activation analysis. The total ion beam charge that passes through the target is three microCoulombs ( $\mu\text{C}$ ) and corresponds to an average ion beam current of 10 nanoamps ( $10^{-8}\text{ A}$ ) for 300 seconds.

**Table 4.1.** Comparison of the measured PIXE values with the nominal values for six Micromatter standard filters for each month in 1992.

Measured/ Nominal Concentration PIXE 1992									
Date	#Runs	Al	Si	Cl	Ca	Fe	Sr	Mean	StDev
Jan-92	184	1.026	0.957	1.002	1.008	1.026	0.977	0.999	0.028
Feb-92	220	1.035	0.970	1.010	1.014	1.028	0.956	1.002	0.032
Mar-92	224	1.026	0.967	1.004	1.016	1.021	0.974	1.001	0.025
Apr-92	287	1.014	0.944	0.999	1.021	1.031	0.974	0.997	0.033
May-92	248	1.004	0.948	1.014	1.038	1.039	0.981	1.004	0.035
Jun-92	248	1.007	1.007	0.963	0.998	0.989	1.034	0.999	0.023
Jul-92	305	1.021	0.962	1.018	1.027	1.033	0.976	1.006	0.030
Aug-92	263	1.019	0.937	1.003	1.014	1.024	1.003	1.000	0.032
Sep-92	253	1.005	0.942	1.052	1.009	1.019	0.972	0.999	0.038
Oct-92	309	1.034	0.954	1.037	1.016	1.008	0.972	1.003	0.034
Nov-92	260	1.003	0.956	1.037	1.016	1.011	0.979	1.000	0.029
Dec-92	324	1.012	0.948	0.999	1.028	1.022	0.999	1.0015	0.029
1992 Av.	3125	1.017	0.958	1.012	1.017	1.021	0.983	1.001	0.028

The characteristic peak areas from the PIXE spectra are fitted by the computer codes at ANSTO. To convert these to elemental concentrations on the filters and then to atmospheric aerosol concentrations, the calibration constants and the cyclone filter areas and through-put volumes during the 24 hour sampling period are necessary. The conversions from peak areas to filter concentrations per unit area are obtained by running known Micromatter standard filters at the beginning and end of each analysis run on the accelerator. These standard filters are commercially available and have known elemental concentrations deposited on them, with an accuracy of  $\pm 5\%$ . Al, Si, Cl, Ca, Fe and Sr standards were used to calibrate detection efficiencies. The results for the comparison of these standards with the measured values, for each month during 1992, are shown in Table 4.1. For the 3125 runs analysed during 1992 all six Micromatter standards showed excellent reproducibility with standard deviations well within the nominal  $\pm 5\%$  quoted by the supplier. The mean measured to nominal ratio for the year was  $(1.001 \pm 0.028)$  showing the high accuracy and good precision of the PIXE calibration measurements.

#### 4.1.2 Particle Induced Gamma-ray Emission (PIGME)

For sufficiently high ion beam energies the interaction of the ions with the nuclei of the target atoms may produce gamma rays. These gamma rays have energies from a few hundred keV to several MeV and in a manner totally analogous to X-ray production discussed above, the energy of the gamma ray determines the element nuclei hit by the incoming ion beam. The number of gamma rays detected is a function of the concentration of this element in the target. PIGME analysis is typically used to detect Li, Be, B, F, Na, Mg, and Al elements in a sample. Hence the PIGME technique is ideally suited to complement the PIXE results for elements below silicon where the X-ray detection efficiency for PIXE falls very rapidly, making measurements of light elements up to aluminium extremely difficult. This is one of the main reasons that PIGME and PIXE spectra are acquired simultaneously on the same filter sample (Cohen 1992). However, because PIGME originates from a nuclear process rather than an atomic reaction it is significantly less sensitive for aerosol filter analyses than PIXE. For all filters from the ERDC network PIGME was used for analyses of fluorine and sodium on the Teflon filters. The sodium originates from seaspray and windblown soil and the fluorine is the major constituent (76% by weight) of Teflon and so this measurement can be used to monitor the Teflon filter thickness (typically  $224 \pm 19 \mu\text{g}/\text{cm}^2$ ).

Figure 4.4 shows a typical PIGME spectrum for a filter from the Cape Grim (ASP25) site in north western Tasmania for the 16 August 1992. This spectrum was obtained simultaneously with the equivalent PIXE spectrum using 2.6 MeV protons and a total accelerator run time of a few minutes (3  $\mu\text{C}$  of charge). The lower plot shows the region from 0 to 700 keV showing the Na 440 keV gamma ray in more detail. As with the PIXE spectra the sharp peaks are characteristic of the elements present and their areas are proportional to the elemental concentrations. Cape Grim is a coastal site so there is a reasonable amount of Na present in the aerosol (2083  $\text{ng}/\text{m}^3$  of air). Each element may have several identifying peaks, for example fluorine has gamma ray peaks at 197 keV and 3 other peaks between 5100 and 6130 keV, all of which could be used for analysis if required. The low energy 197 keV peak is used as it has a better signal to noise ratio than the higher energy peaks. The sodium is analysed using the gamma ray peak at 440 keV. It sits on a reasonably large gamma ray background but still returns with sufficient sensitivity to detect sodium above about 140  $\text{ng}/\text{m}^3$  of air for a 24 hour average. Peaks from other light elements such as Li and Be, are generally not observed as their concentrations are mostly below 100  $\text{ng}/\text{m}^3$  or as is the case with Mg, Al, and Si the sensitivity of the PIGME technique is not sufficient to detect values below a few hundred  $\text{ng}/\text{m}^3$ .

The PIGME technique is calibrated against Micromatter standard foils in the same manner as the PIXE method. The standard filters used are thin evaporate targets of sodium chloride, calcium and strontium fluoride. The standard deviations for sodium and fluorine yields for all 3125 runs analysed during 1992 were  $\pm 8\%$  and  $\pm 7\%$  respectively, showing the precision of the PIGME technique, like its sensitivity, is less than the PIXE method (3%), but acceptable for aerosol analysis work.

#### 4.1.3 Particle Elastic Scattering (PESA)

Particle elastic scattering (PESA) involves an incoming ion beam elastically scattering off target nuclei and their energies being detected as a means of identifying the target nuclei struck. For a proton beam traversing a thin target, such as an aerosol filter paper, this technique becomes particularly suited for hydrogen analysis. The principles of the technique are schematically shown in Figure 4.5 where 2.6 MeV protons are incident normally onto a 25  $\mu\text{m}$  thick (220  $\mu\text{g}/\text{cm}^2$ ) Teflon filter. If the detector is placed at small forward scattering angles ( $\sim 30^\circ$ ) it will receive a range of scattered proton energies. The kinematics of the scattering process are such that for elements heavier than hydrogen,

such as the carbon and fluorine in the Teflon filter, protons of higher scattered energy are produced and the idealised spectrum displayed at the bottom of Figure 4.5 results. Hydrogen being the lightest element has a unique signature, shown as the edges (a)-(b), at the lowest scattered proton energies. Other heavier elements produce the edges (c)-(d), at higher scattered proton energies, shown in Figure 4.5 and are generally not resolved.

Figure 4.6 shows the PESA spectra for the Teflon filters whose PIXE spectra are shown in Figure 4.2. Despite the presence of many elements heavier than fluorine (Na, Al, Si, S, Ca, Fe, Zn, Pb, Br, etc.) the hydrogen peak of Figure 4.6 is still well resolved and corresponds to a mass of several  $\mu\text{g}/\text{cm}^2$  on the filters. The area of the background subtracted hydrogen peak of Figure 4.6 is linearly proportional to the hydrogen concentration in the filter over the concentration range 0-200  $\mu\text{g}/\text{cm}^2$  (Cohen 1992). The PESA measurements are performed in vacuum, so all free water vapour and volatile hydrocarbons evaporate off the filter. Weighing tests described above show that these vacuum losses are generally less than 8% of the total fine particle mass on the filters (see Figure 4.12).

Thin Mylar foils (6  $\mu\text{m}$ ) which contain 35  $\mu\text{g}/\text{cm}^2$  of hydrogen are used to calibrate the PESA system at the beginning and the end of each analysis run every month. The standard deviation of these calibrations over the twelve month period January to December 1992 was  $\pm 9\%$  showing that the precision of the PESA technique is quite good. Furthermore a calibration constant of around 650 counts/ ( $\mu\text{gcm}^{-2}$ )/ 3  $\mu\text{C}$  run provides high sensitivities for this technique of the order of 15  $\text{ng}/\text{m}^3$  of air.

#### 4.1.4 Rutherford Backscattering (RBS)

For proton beam scattering off target nuclei heavier than hydrogen the kinematics allows a small fraction of the beam to be elastically scattered at large backangles greater than  $90^\circ$ . This is called Rutherford backscattering and by placing a detector at scattering angles of  $169^\circ$  we measure the energy of these scattered protons and then calculate the mass of the target atom struck. For input ion beam energies below the target-ion Coulomb barrier (several MeV) the processes are well characterised. We use this IBA technique to measure the total carbon, nitrogen and oxygen concentrations in the filter. A typical spectrum obtained from a Teflon filter is shown in Figure 4.7. Again readily resolved characteristic peaks are obtained for the elements carbon, nitrogen, oxygen and fluorine and the area of these peaks is related to the concentration of the element

present. However, fluorine has several characteristic peaks which reflect several different types of nuclear reactions that can occur at the proton energies used. These other fluorine peaks lie under the nitrogen and oxygen peaks and interfere with them making the background subtraction under these peaks uncertain and introducing systematic errors into the absolute concentration estimates for these elements. The smaller nitrogen peak, between carbon and oxygen is particularly affected by this problem.

Carbon is a major component of Teflon (24% by weight) hence the contribution from the Teflon filter has to be subtracted out before the total carbon content of the particle matter can be estimated. This is done by assuming that Teflon is  $(CF_2)_n$  and using the PIGME fluorine measurement to calculate the carbon content of each filter and then subtracting this from the total carbon content measured by RBS. Typically the 220  $\mu\text{g}/\text{cm}^2$  Teflon filters were loaded with 110  $\mu\text{g}/\text{cm}^2$  of total fine particle matter. On average, 23% was 'Organics' as calculated from PESA, 23% was elemental carbon or soot as measured by LIPM, 23% 'Ammonium sulphate' and 5.7% 'Soil' as measured by PIXE (see below). The average organic particle was assumed to be 9% hydrogen, 20% oxygen and 71% carbon (Eldred et al 1990) and 'Soil' is 56% oxygen as calculated from its common oxide components (see below). Consequently it is expected that the average total carbon and oxygen content of the filters will be around 39% and 19% respectively of the total particle mass. This means the contributions to the total carbon content using RBS for the Teflon filter and the fine particle mass are about 1 to 1. These problems with carbon in the Teflon filters themselves and the interferences from the fluorine peaks make the absolute C and O concentration uncertain to at least  $\pm 30\%$  and more for the smaller N peaks. RBS is not used to estimate the fluorine concentrations on the filters. This is better done using the PIGME analysis as the yields are more consistent and less dependent on the ion beam energy.

Calibration of the C, N and O analyses by RBS was done using standard thickness Mylar (for C and O) and Kapton foils (for N). The precision of these measurements during 1992 was C  $\pm 6\%$ , N  $\pm 9\%$  and O  $\pm 4\%$ . This means that relative C, N, and O measurements should be quite reliable even if systematic errors may mean that absolutely, these concentrations could be more than 30% in error.

#### 4.1.5 Laser Integrated Plate Methods (LIPM)

In appendix A, section A.1, the concepts of visual range (Equation A.1) was discussed and the coefficient of extinction  $b_{ext}$  (Equation A.2) defined. Table A.1 showed that light absorption was most effective for fine particles ( $< 2.5 \mu\text{m}$  diameter) with elemental carbon or soot accounting for 75% or more of the fine particle absorption and 10 - 30% of the total extinction (Sloane et al, 1991). Hence a measure of the absorption coefficient  $b_{ap}$  for particles is also a measure of the elemental carbon content of the aerosol. In 1973 Lin et al described a laser integrated plate technique for measuring the coefficient of optical absorption and more recent work was carried out by Rosen et al 1980 to establish this as a routine technique. The ERDC project used the LIPM technique to measure  $b_{ap}$  on the fine particle Teflon filters.

The LIPM system is shown schematically in Figure 4.8. Light from a HeNe laser of wavelength 633 nm is diffused and collimated to give a uniform beam at the filter. The light transmitted through the filter is collected with a photodiode system. Because of the high opacity of the Teflon filters and the variation in filter thickness it is necessary to measure the transmission of each filter both before and after exposure. The coefficient of absorption of particles ( $b_0$ ) is determined from these two transmission measurements, the area of the deposit on the filter and the volume of air sampled by,

$$b_0 = 100 \cdot \left[ \frac{A}{V} \right] \ln \left[ \frac{I_0}{I} \right] \quad \mu\text{m}^{-1} \quad (4.1)$$

where  $A$  = area of the filter exposed ( $\text{cm}^2$ ),  $V$  = volume of air passed through the filter ( $\text{m}^3$ ),  $I_0$  is the unexposed intensity and  $I$  is the exposed transmission intensity and  $b_0$  is measured in  $\mu\text{m}^{-1}$ . The coefficient of absorption  $b_0$  calculated from Equation 4.1 needs to be corrected for layering of the aerosol on the filter, especially for heavily loaded filters as may occur in industrial areas. Eldred 1993 makes the following layering corrections to all their filters in the US IMPROVE network,

$$b_{ap} = 0.97 \cdot \frac{b}{R} \quad (4.2)$$

where,

$$R = 0.36 \cdot \exp\left[\frac{-\rho t}{22}\right] + 0.64 \cdot \exp\left[\frac{-\rho t}{415}\right] \quad (4.3)$$

$\rho t$  = the thickness/unit area of the particle on the filter in  $\mu\text{g}/\text{cm}^2$  and is typically  $100 \mu\text{g}/\text{cm}^2$  for the ERDC network. The factor 0.97 is a correction for large angle scattering determined by comparison of an integrating plate and an integrating sphere. The layer correction  $R$  is always less than unity and has been plotted as a function of fine particle loading in Figure 4.9. For the mean 1992 fine particle mass of  $107 \mu\text{g}/\text{cm}^2$  the correction factor  $R=0.50$ , generally for all the sites in our network  $0.3 < R < 0.7$ .

Studies by the University of California (Eldred 1993) have shown that the layer correction as defined by Equation (4.3) is a reasonable estimate. They ran two sampling modules along side one another with collection areas differing by a factor 2 and compared their layer corrections. They found that with no layer correction the absorption coefficient with higher mass density was  $(0.75 \pm 0.10)$  of that with lower mass density. With the  $R$  correction above the two measurements were closer, with a slope of  $(0.94 \pm 0.12)$ .

The elemental carbon or soot is responsible for around 30% of the total light extinction and often more than 90% of the light absorption by particles (Groblicki et al 1981, Appel et al 1985, Japor et al 1986). It can therefore be estimated from the measurement of  $b_{ap}$  by,

$$Elt.C = 1000 \cdot \left[ \frac{b_{ap}}{\varepsilon} \right] \text{ ng / m}^3 \quad (4.4)$$

where  $\varepsilon$  is the absorption efficiency in  $\text{m}^2/\text{g}$ ,  $b_{ap}$  is in  $\mu\text{m}^{-1}$  and the elemental carbon (Elt.C) is in  $\text{ng}/\text{m}^3$ . Elemental carbon will also sometimes be referred to in this report as Elt.C, laser carbon or Lcarb as it originates from the laser absorption measurements. Values of the absorption efficiency  $\varepsilon$  vary from around 9 to  $12 \text{ m}^2/\text{g}$  but the generally accepted value for diesel associated carbon is  $\varepsilon = 10 \text{ m}^2/\text{g}$  (Sloane et al, 1991). Table 4.2 is taken from the work of Sloane et al 1991 and shows the relative contributions to the absorption and scattering efficiencies on two days in January 1988 in Denver, USA.

Clearly elemental carbon is the major contributor to the absorption efficiency of fine particles and sulphate, nitrates and organics contribute equally to the scattering

SECTION 4 - ANALYSIS TECHNIQUES

efficiency depending more on the relative humidity (RH) than does the absorption efficiency, (Horvath, 1993).

The average  $b_{ap}$  for the network during 1992 was  $(17 \pm 15) \mu\text{m}^{-1}$ , using a value of  $\epsilon_{ap} = 10 \text{ m}^2/\text{g}$  and Equation (4.4) it is found that the average elemental carbon for 1992 was  $1740 \text{ ng}/\text{m}^3$  or 23% of the fine particle mass, consistent with US findings, (Malm et al, 1994).

The minimum detectable limit for the LIPM system is around  $0.2 \mu\text{m}^{-1}$ , which corresponds to a 3% change in  $[I_0/I]$  in Equation (4.1). This is well below our typical value of  $17 \mu\text{m}^{-1}$ . The precision of the elemental carbon estimates is dominated by the error in the layered correction factor R. Figure 4.9 shows that this is largest for light loadings where the total mass is less certain. It is estimated that for the lightly loaded filters ( $< 30 \mu\text{g}/\text{cm}^2$ ) R has an error of 8% and for the heavily loaded filters ( $> 200 \mu\text{g}/\text{m}^2$ ) this error reduces to 3%, giving a 4 to 9% error in the precision of  $b_{ap}$  and the estimate of the elemental carbon.

**Table 4.2.** The absorption efficiency  $\epsilon_{ap}$  and scattering efficiency  $\epsilon_{sp}$  for various components of the fine mass for 2 days in January 1988 in Denver, USA, taken from the work of Sloane et al 1991.

Species	5 January 1988 74% RH., NE Winds			13 January 1988 38% RH., No Wind		
	FPM ( $\mu\text{g}/\text{m}^3$ )	$\epsilon_{ap}$ ( $\text{m}^2/\text{g}$ )	$\epsilon_{sp}$ ( $\text{m}^2/\text{g}$ )	FPM ( $\mu\text{g}/\text{m}^3$ )	$\epsilon_{ap}$ ( $\text{m}^2/\text{g}$ )	$\epsilon_{sp}$ ( $\text{m}^2/\text{g}$ )
FPM	54.6	1.7	4.5	51.3	1.9	2.3
SO <sub>4</sub>	5.4	0.6	6.8	2.2	0.3	2.0
NO <sub>3</sub>	13.9	0.4	6.6	16.1	0.3	2.3
Organ. C	13.4	0.3	5.6	16.4	0.7	4.0
Elt. C	7.5	10.2	1.6	8.8	10.2	0.9

The absolute accuracy of the LIPM system for elemental carbon estimates is a little less uncertain and comparison of this technique with thermal optical reflectance (TOR) measurements have been made over the years (Groblicki et al 1981, Cadle and Groblicki 1981, Johnson et al 1981, and Sloane et al 1991). In TOR the temperature of the sample is raised in steps from ambient to 800°C. During the initial steps up to 550°C, the atmosphere is 100% helium. During the 550°C step, 2% O<sub>2</sub> is introduced and maintained. During the entire time, evolved CO<sub>2</sub> and the reflectance of the sample is measured. It is assumed that no elemental carbon is evolved in a pure helium atmosphere. When the sample is heated above 120°C, the reflectance decreases, presumably because of an increase in the coefficient of absorption. It is thus assumed that some organic is pyrolysed and remains on the filter as elemental carbon, this is evolved when O<sub>2</sub> is introduced during the 550°C step. Therefore any carbon evolved in O<sub>2</sub> before the reflectance returns to the initial value is assumed to be pyrolysed organic carbon and not elemental carbon. These TOR steps are summarised in Table 4.3.

In the TOR method all the CO<sub>2</sub> evolved until the initial reflectance is regained is considered organic (OC1+ OC2+ OC3+ OC4+ P). The remainder (EC1+ EC2+ EC3) is considered elemental carbon. The latter quantity has been found not to correlate well with the elemental carbon from LIPM (Sadler et al 1981, Japor et al 1986) and to be out by a factor of 2. However recent measurements by the US IMPROVE group (Eldred 1993) in conjunction with Huffman and Malm from the Fort Collins USEPA group have shown that by comparing  $b_{ap}$  with different groupings of carbon listed in Table 4.3 good correlations are obtained.

The best correlations were obtained with the sum of the components (OC4+P+EC1+EC2) and  $b_{ap}$ . That is the sum of all carbon evolved between 450°C and 700°C. They also found poor correlations of  $b_{ap}$  with the highest temperature EC3 (above 700°C). When  $b_{ap}$  was compared to this new carbon variable (450-700°C) the absorption efficiency was found to be 10 m<sup>2</sup>/g obtained with diesel studies.

**Table 4.3.** Summary of the steps used in standard thermal optical reflectance (TOR) measurements, after Eldred 1993.

Temperature (°C)	Atmosphere	Reflectance	Label
Ambient - 120	100% He	Begins to decrease	OC1
120 - 220	100% He	Decreases further	OC2
220 - 450	100% He	Decreases further	OC3
450 - 550	100% He	Increases sharply	OC4
550	2% O <sub>2</sub>	Reaches initial value again	P
550	2% O <sub>2</sub>		EC1
550 - 700	2% O <sub>2</sub>		EC2
700 - 800	2% O <sub>2</sub>		EC3

#### 4.1.6 Minimum Detectable Limits (MDL) and Errors

To determine the minimum detectable limits for the 25 or so elements measured the background under each elemental peak (in the typical plots shown in Figures 4.2, 4.4, 4.6 and 4.7) was considered for each of the analysis techniques used. The minimum detectable limit (MDL) for a given element is defined as  $3.29C \cdot \sqrt{B}$  where B is the background counts under the peak in the spectrum and C is the conversion constant from counts to ng/m<sup>3</sup> for that element (Clayton 1986). This is a very conservative estimate of the MDL and takes into account interelement interferences. Figure 4.10 shows the results of such a calculation for all techniques and for the trace elements measured by the ERDC network. The PIXE technique utilises two characteristic X-ray lines, the K series and the L series lines. The K lines cover light elements between Al and Zr (atomic numbers 13 to 40) and the L lines the heavier elements between Dy and Pb (atomic numbers 66 to 82) with MDL's lower than 10 ng/m<sup>3</sup>. the PIGME technique is used for Na and F with MDL's of 180 and 350 ng/m<sup>3</sup> respectively and C, N and O RBS sensitivities lie between 100 and 400 ng/m<sup>3</sup>. Hydrogen from the PESA technique is measured with a sensitivity of 21 ng/m<sup>3</sup> and the elemental carbon by LIPM with an MDL of 3 ng/m<sup>3</sup>. Elements between Zr and Dy (atomic numbers 40 to 66), such as the rare earths, have sensitivities between 10 and 100 ng/m<sup>3</sup>. However these occur naturally in

SECTION 4 - ANALYSIS TECHNIQUES

the study area at levels several orders of magnitude below this and consequently are not detected by these techniques. The average minimum detection limits of around 10 ng/m<sup>3</sup> for the majority of elements is more than sufficient for most components in Sydney aerosols and is several orders of magnitude below the typical fine mass loadings on the filters.

The precision in each concentration is calculated as a function of statistical counting or accumulation errors and experimental or measurement errors. The experimental errors tend to be relatively constant and are best estimated by regular measurements of known standards. Whereas errors due to statistical counting depend on the concentration of a given element on a given day at a given site, with high concentrations obviously having lower associated errors. Table 4.4 shows the experimental errors obtained for each analysis technique used for the network during 1992. We see that this error is typically between 5 and 10%.

**Table 4.4.** Typical experimental errors for all analysis techniques used in the ERDC network during 1992.

Technique	Error	Comments
Weight	3-5%	Depends on the mass loading
PIXE	3%	Measured on standards over 12 months
PIGME	7-8%	Measured on standards over 12 months
PESA	9%	Measured on standards over 12 months
RBS	4-9%	Measured on standards over 12 months
LIPM	4-9%	depends on the mass loading

The error associated with each individual element concentration depends on the counting statistics for that element. Elements with concentrations near their MDL's will by definition have counting errors of around 100%. For example cobalt typically occurs at around 0.5 ng/m<sup>3</sup> throughout the network which is comparable with its MDL, whereas

SECTION 4 - ANALYSIS TECHNIQUES

sulphur has an average value of over 400 ng/m<sup>3</sup> which is 170 times its MDL. The statistical counting errors associated with these two elements were calculated to be 117% and 1% respectively. Table 4.5 shows the statistical counting errors for each of the elements analysed. It was calculated from the analysis of over 1000 typical filters acquired from all 25 sites during 1992 and includes peak area and background subtraction errors. The term RCM is the reconstructed mass defined below under pseudo elements and represents the sum of all elemental components for comparison with the total fine particle mass. Finally the total error on each elemental measurement is obtained by assuming the statistical errors and the experimental errors are independent and adding the two in quadrature. This produces errors from a few percent to over 100% depending on the elements measured and this should be kept in mind when quoting elemental concentrations especially for elements like Co which occur at levels near the minimum detectable limit of our system.

**Table 4.5.** Typical statistical counting errors associated with the elemental analysis of 1000 filters obtained from the network during 1992.

Elt	Error %	Elt	Error %	Elt	Error %
Al	20	V	78	Pb	15
Si	5	Cr	61	H	2
P	40	Mn	27	F	5
S	1	Fe	5	Na	5
Cl	16	Cu	24	TOTC	1
K	2	Co	117	TOTN	17
Ca	6	Ni	47	TOTO	6
Ti	32	Zn	14	RCM	6
		Br	16		

## 4.2 FILTERS

The ERDC project has analysed over 5,000 filters and each of these have been subjected to weighing and laser integrated plate techniques before and after exposure, and then to the full IBA analysis techniques described below. Using these techniques it is possible to detect elemental concentrations, down to a few  $\text{ng/m}^3$  of air, of the following elements: H, C, N, O, F, Na, Al, Si, P, S, Cl, K, Ca, Ti, V, Cr, Mn, Fe, Ni, Cu, Zn, Br and Pb. The techniques are also sensitive to other elements such as Se, As, Y, Zr, Ba, Sn, Cd, Ta, W, Hg, and Au. However these were generally below the minimum detectable limits of around  $10 \text{ ng/m}^3$  and hence were not reported in this project. Selected filters from selected sites for both summer and winter times have also been analysed using ion chromatography (IC) and neutron activation analysis (NNA) for comparison with these IBA data.

### 4.2.1 Filter Weighing

The Teflon filters were weighed before and after their 24 hours exposures, to determine the fine particle mass collected. All filters were stored in a temperature and humidity controlled weighing room for a minimum of 24 hours before each weighing. The average total mass collected on all filters, from all sites in 1992 was  $(236 \pm 107) \mu\text{g}$ . The average filter plus support ring weigh around 42 mg, hence the precision of the measurement needed to be better than  $\pm 5 \mu\text{g}$ . A Metler balance calibrated using 20, 50 and 100 mg standard weights was used for all measurements. This balance is capable of weighing to  $\pm 1 \mu\text{g}$  and the instrument's precision for the six months from June to December 1992 was  $\pm 1.5 \mu\text{g}$  (Figure 4.11), sufficient to give better than  $\pm 5\%$  values on the lightest of filter loadings.

The IBA techniques described below require each filter analysis to be carried out inside a vacuum chamber so tests were performed to see if this procedure affected the filter weights. The pre- and post- exposure weighing were both carried out before the filters were analysed in vacuum and so the fine particle gravimetric mass was not affected by this analysis. However, when comparing the fine particle mass as measured on the balance with the sum of all the elemental constituents as measured by the IBA techniques it was necessary to determine if any mass was lost in vacuum. Some mass loss from volatiles (water vapour, ammonium salts, etc.) held in the mesh of the Teflon filter could be expected (Martinsson 1987). Tests by Martinsson on aerosols using ion

beam techniques in vacuum showed typically mass losses to be less than 0.2%/ minute for beam current densities less than 0.5 nA/mm<sup>2</sup>. Since irradiation times in the ERDC project were always less than 5 minutes and current densities less than 0.3 nA/mm<sup>2</sup> it was expected that the loss of volatiles from aerosols during analysis would be minimal.

To test mass losses due to the filter being placed in the vacuum, the filters were weighed 6 times: at least a month before insertion into vacuum; at least a day before insertion into the vacuum; immediately after removal from vacuum, and a further 3 times (ranging from several days to more than a week after removal from the vacuum).

The results for 10 filters with average mass loadings (210 µg) and 5 filters with higher mass loading (265 µg) are shown in Fig. 4.12 for tests performed in January 1992. The weights were normalised to the first weighing and the standard deviations for each of the 6 times are shown on the plots. The solid curve is for temperature but no humidity control in the weighing room and the dashed curve is corrected for constant humidity. There appears to be a slight drop in the weight of the filters of around 8% immediately after removal from the vacuum, but with temperature and humidity control the filters return to their original weight within 48 hours. These results are consistent with similar experiments performed at the University of California, Davis (Wilkinson 1993) on similar Teflon filters where they found decreases of around 5% of weight in vacuum. These also returned to the original weights after a day or so at normal pressures.

### 4.3 PSEUDO ELEMENTS AND COMPOSITE VARIABLES

The ion beam analysis techniques used in the ERDC project detect elemental concentrations. Table 2.1 showed that many of these elements can fingerprint a variety of different fine particle sources. It is interesting to combine some of these elements to try and estimate concentrations of compounds of known chemical composition. For example the major constituent of seaspray is NaCl. Both these elements are measured so it should be possible to put together a composite variable which is representative of the seaspray component of our fine aerosol. Windblown soils can be expected to be composed of oxides of the elements Al, Si, Ca, Ti and Fe which make up some of the major elements present in soil. Again a composite variable can be made that approximates the fine soil components of the aerosols. Other combinations of pure elements that represent signatures for interesting aerosol components can be derived. These are denoted 'pseudo-elements'. For example, fine K is a known indicator for

smoke from wood combustion. However potassium also occurs as an oxide in soils. If another element such as Si or Fe is used as a tracer for soil and the soil component subtracted out from the total K measurement, the result would be a pseudo element representative of smoke.

The University of California, Davis have used these composite variables and pseudo-elements to describe the aerosol measurements from the IMPROVE network (Cahill et al 1989, Eldred et al 1990 and Eldred and Cahill 1991). The ERDC project has followed this system closely and has defined the following composite variables and pseudo-elements to help gain a better understanding of the possible sources and their contributions to the average ambient aerosol throughout the network.

#### 4.3.1 Sulphate

Sulphur is one of the major elemental components measured by the network and sulphate is a recognised major component of fine aerosols. Sulphur primarily enters the atmosphere as SO<sub>2</sub> gas and is slowly converted to sulphuric acid (H<sub>2</sub>SO<sub>4</sub>), which is then neutralised by ammonia gas to form ammonium hydrogen sulphate NH<sub>4</sub>HSO<sub>4</sub> or ammonium sulphate (NH<sub>4</sub>)<sub>2</sub>SO<sub>4</sub> depending on the degree of neutralisation. The rate of this transformation depends on the amount of ammonia gas and water vapour in the air. Using the atomic weights of each of these chemical species we can define the pseudo-elements for the sulphate ion in its various forms from the elemental sulphur concentration. This is shown in Table 4.6.

Sulphate ions represent the thermodynamically stable form of particulate sulphur in the atmosphere. Metal sulphides (from stockpiles of ores around smelters) and elemental sulphur (around sulphuric acid plants) are the two other forms of particulate sulphur which may be present; but these occur in predominantly as particles with aerodynamic diameters greater than 2.5 µm and thus be small contributors to fine particles.

When sulphate ions are initially formed in the atmosphere by oxidation of sulphur dioxide in the gas-phase, in water droplets or in surface-catalysed processes, hydrogen ions are the counterions. The aerosol particles are strongly hygroscopic and, under the usual conditions of humidity, would occur as tiny aqueous droplets ("sulphuric acid" aerosol). The hydrogen ions in the aerosol are slowly neutralised by basic materials. The most abundant natural base is ammonia, which arises from denitrification processes in the soil. Under natural conditions, the acid aerosol would be progressively neutralised by

**Table 4.6.** The definition of pseudo elements SO<sub>4</sub>, NHSO<sub>4</sub>, NHSO<sub>4</sub>bi and H<sub>2</sub>SO<sub>4</sub> from the elemental sulphur concentrations S.

Form	Definition	Neutralisation	Comments
SO <sub>4</sub> <sup>2-</sup>	SO <sub>4</sub> = 3.000*S	-	Sulphate ion remote, urban sites urban, industrial sites heavy industrial sites and Arctic or Antarctic (no NH <sub>3</sub> )
(NH <sub>4</sub> ) <sub>2</sub> SO <sub>4</sub>	NHSO <sub>4</sub> = 4.125*S	100%	
(NH <sub>4</sub> )HSO <sub>4</sub>	NHSO <sub>4</sub> bi = 3.594*S	50%	
H <sub>2</sub> SO <sub>4</sub>	H <sub>2</sub> SO <sub>4</sub> = 3.063*S	0%	

ammonia, forming ultimately a solution of ammonium sulphate. The intermediate stage of ammonium hydrogen sulphate is sometimes present, but the process of neutralisation is a continuous one with all ratios of H<sup>+</sup> to NH<sub>4</sub><sup>+</sup> ions possible.

Other bases besides ammonia can neutralise the aerosol. Wood burning produces potassium carbonate ("potash") and the carbonate ions in this material would readily react with aerosol acidity, leaving potassium ions as the counterions for the sulphate. Ash from coal combustion is usually alkaline, containing calcium carbonate, calcium hydroxide, basic magnesium salts, potassium carbonate, iron oxides and other metal oxides; after these materials have reacted with acidic aerosols, calcium, magnesium, iron and other metal ions remain as counterions.

The combustion of leaded petrol in Sydney produces PbBr<sub>2</sub>, PbBrCl, PbBrCl.2NH<sub>4</sub>Cl and 2PbBrCl.NH<sub>4</sub>Cl which, on reaction with sulphur dioxide or acid sulphate aerosols in an urban atmosphere, yield PbBrCl.(NH<sub>4</sub>)<sub>2</sub>SO<sub>4</sub>, PbBrCl.(NH<sub>4</sub>)<sub>2</sub>BrCl and PbSO<sub>4</sub> (with loss of HCl or HBr). In areas contaminated with exhaust products from motor vehicles, a combination of lead and ammonium ions may act as counterions for sulphate in some particles.

When urban aerosol particles are collected on Teflon filters, particles which were formerly separate are brought together. Substantial loss of nitrate ions is known to occur through evaporation of nitric acid, removing hydrogen ions from the filter. Other reactions between hydrogen ions and compounds in solid particles would also be facilitated.

Metallurgical "fume" (from pyrometallurgical processes) may contain fine particles of metal oxides resulting from gas-phase condensation. When sulphur dioxide is either produced simultaneously or released as a result of nearby processes, it is likely that the metals in the fume contribute to the cations associated with sulphate ions. Cations which might be contributed in this way, for example around the copper smelter at Port Kembla, are zinc, lead and cadmium (Archibold and Crisp, 1983).

The cations associated with sulphate ions in the fine aerosol particles have been determined for a few percent of filters in this study. Determination of ammonium ion concentrations would be especially useful and will be the subject of further work. Since the ammonium salts on the filters are stable at least in the short term and the ion beam analysis techniques are non-destructive, it will be possible to carry out these analyses at a later time.

Indirect information is available from the ERDC study concerning the counterions associated with sulphate. Since the beginning of 1993, concentrations of nitrogen has been directly determined by RBS (see section 4.1.4). The values for nitrogen are subject to a higher degree of uncertainty ( $\pm 30$  to 50%) than that for other elements (typically  $\pm 5$  to 10% at  $>3$  times the minimum detectable limit). The relationship between sulphur and nitrogen concentrations at Muswellbrook (Figure 4.13), a country site receiving relatively high levels of airborne sulphates, is consistent with complete neutralisation of aerosol acidity by ammonia if all of the nitrogen in particles at this site is in the form of ammonium ions (mass ratio S/N = 1.14). However, some nitrogen will certainly be present as nitrate ions (derived from nitrogen oxides from high-temperature combustion processes), and neutralisation may not be complete. A similar plot using data for all sites is given in Figure 4.14 for the summer months. The line through the data is consistent with 100% neutralisation of sulphate aerosols by ammonia. Points above the line correspond to less than 100% neutralisation and points below to excess nitrogen not associated with sulphur. Work by Ayers et al 1987 showed that Sydney's rainwater is more acidic during summer than during the winter this study supports this hypothesis particularly for high sulphur values during summer months.

It has been assumed for simplicity that the sulphate is completely neutralised by ammonia to form ammonium sulphate. This allows mass balances to be calculated, and these balances will only be marginally affected (by a few percent) if the degree of neutralisation proves to be lower. It also allows the pseudoelement concept to be used to visualise the composition of the particles. It should be borne in mind, however, that the pseudoelement 'ammonium sulphate' used throughout this report assumes all the sulphate is fully neutralised. This may need revision when further data become available.

For the Wollongong/ Sydney/ Newcastle region the sulphate ion occurs on the filters as mainly ammonium sulphate or ammonium hydrogen sulphate. This is demonstrated in Figure 4.15 where the sulphur concentration is plotted against the hydrogen concentration for all sites in the network for 1992. There is a clear cutoff at the line representing a (S/H)=4 ratio for ammonium sulphate with no data falling between this line and the line for sulphuric acid (S/H)=16. Most of the data points lie on or to the right of the (S/H)=4 line for ammonium sulphate because the excess hydrogen occurs in forms not associated with sulphur such as in organics or water vapour. This plot is not evidence that there was no sulphuric acid aerosol in the atmosphere over the sampling region during 1992. It says that if the atmosphere aerosol was acidic then it became neutralised while residing on the filter before analysis. To confirm the acidity of the atmospheric aerosol one would need to measure the ammonium ion concentration independently.

The definitions of Table 4.6 have been tested by comparison with independent  $\text{SO}_4^{2-}$  measurements using ion chromatography and the sulphur measurements using PIXE. The agreement is excellent with the  $(\text{SO}_4^{2-}/\text{S})$  ratio being 3.0 with a correlation coefficient of  $R^2=0.885$ . This is discussed further in section 4.4. The average sulphur concentration for all sites for 1992 was 5.6% of the fine particle mass. If it is assumed this occurred as fully neutralised ammonium sulphate, 'Ammonium sulphate' would have been 23% of the fine particle mass in 1992.

Future references to ammonium sulphate in this report will use single quotes when referring to fully neutralised sulphate ions as defined in Table 4.6 using the measured sulphur concentration.

### 4.3.2 'Salt'

Sea salt is composed mainly of sodium (32% by weight.) and chlorine (58%) with minor components of Mg (4%), S (3%), Ca (1%), K (1%) and Br (0.25%) (Weast 1977). Sodium chloride represents 90% of the dried weight of sea water so it is useful as an indicator of sea spray components in our fine particles. All of the elements listed above, except Mg, were measured by the ERDC project. We define the pseudo-element representative of sea salt as a multiple of the measured sodium concentration, namely;

$$\text{'Salt'} = 2.54 * \text{Na} \quad (4.5)$$

This equation assumes all of the sodium in the aerosol is associated with sea salt as sodium chloride. There is some sodium oxide in soils, about 1% (Weast 1977). However this correction applied to Equation (4.5) is less than 2% since the average sodium concentration in our aerosols (3%) is about half the average soil concentration (6%). We do not use chlorine in estimating the sea salt component because additives in Sydney petrol are also a significant source of chlorine. Furthermore chlorine may be lost from the filter in acidic environments.

Future references to salt or seaspray in this report will use single quotes when referring to salt defined by Equation (4.5) using the measured sodium concentration

### 4.3.3 'Soil'

Windblown soil is composed mainly of the oxides of Mg, Al, Si, Ca, Ti and Fe with obviously many other trace elements. Weast 1977 gives the average composition of sandstone and sedimentary rocks and the summation of the 5 major oxides of Al, Si, Ca, Ti, and Fe accounts for more than 85% of the total composition. The major exclusions being MgO, Na<sub>2</sub>O, K<sub>2</sub>O and water. In order to put together a composite variable that represents soil and flyash in our aerosols, fine 'soil' is defined as the summation of these 5 oxides with a multiplicative factor of 1.16 to compensate for the exclusion of the other 3 oxides and water, This exclusion factor of 1.16 is calculated from the expected abundance of these oxides in sedimentary soils (Weast 1977). That is,

$$\text{Fine 'Soil'} = 2.20 * \text{Al} + 2.49 * \text{Si} + 1.63 * \text{Ca} + 1.94 * \text{Ti} + 2.42 * \text{Fe} \quad (4.6)$$

This equation also assumes that the two common oxides of iron  $\text{Fe}_2\text{O}_3$  and  $\text{FeO}$  occur in equal proportions. The factor of 2.42 for iron also includes the estimate for  $\text{K}_2\text{O}$  in soil through the  $(\text{K}/\text{Fe})=0.6$  ratio for sedimentary soils. For 1992 the average fine 'soil' concentration for all sites was around 6% of the total fine particle mass.

Future references to soil in this report will use single quotes when referring to soil as defined in Equation (4.6) using the measured elemental concentrations.

#### 4.3.4 'Smoke'

As previously mentioned fine potassium is an accepted indicator for smoke from wood burning and bush fires. In order to obtain a reliable smoke indicator from the fine potassium it is necessary to first subtract the fine potassium associated with soil. Weast 1977 gives a ratio of  $(\text{K}/\text{Fe}) = 0.6$  for sedimentary soils. Plots of K against Fe for rural sites like Oberon (ASP13) and Putty (ASP16), when there was little or no smoke present, confirm this ratio for fine soil aerosols (with no industrial component) in the network. Hence we define the pseudo element smoke which is obtained from the measured total fine potassium with the potassium associated with soil removed. That is:

$$\text{'Smoke'} = (\text{K} - 0.6 \cdot \text{Fe}) \quad (4.7)$$

This parameter has the potential to give a negative result in non smoky areas, or in industrial areas like Wollongong or Newcastle where the Fe content of the aerosol is in excess of the expected Fe content of natural soil in the area. However this parameter has been tested at sites that have been shut down by smoke from bush fires and found it to be a very sensitive indicator of smoke when the fine potassium levels exceed the expected fine potassium from natural soil. It is a good parameter for monitoring wood burning in metropolitan areas during the winter times and it increases by factors of 2-5 between summer and winter seasons at some sites.

Future references to smoke in this report will use single quotes when referring to smoke and/ or ash as defined in Equation (4.7) using the measured fine potassium and iron concentrations.

#### 4.3.5 'Organic Matter'

Organic matter was a major component of the fine aerosols measured. Work by Cadle et al 1983 and Hering 1987 have shown that the measurements made on quartz filters are subject to a major artifact, retention of organic gases. Cahill et al 1989 have estimated organic matter by two methods using chemically inert Teflon filters from 34 sites from their US network during 1982-1987. The two techniques used were the remaining mass method, based on the difference between the measured mass and the sum of all measured components and the nonsulphate hydrogen method. The ERDC network uses similar Teflon filters to the Cahill study and the second method or nonsulphate hydrogen technique was used to estimate fine particle organic matter. This was done because the hydrogen PESA technique for measuring the total hydrogen content on filters had good precision and accuracy. In this technique it is assumed that: (a) the total hydrogen on the filter as measured by PESA is composed mainly of hydrogen from organic material and hydrogen from ammonium sulphate (assumes the sulphate ion is fully neutralised), (b) hydrogen in water is removed in vacuum during analysis, (c) hydrogen in nitrates is not well retained by Teflon filters (Eldred et al 1989) and hence negligible and (d) the hydrogen content of soils is also negligible (Weast 1977).

Furthermore, the average 'Organic matter' is assumed to be composed of 9%H, 71%C and 20%O by weight (Eldred et al 1990 and Eldred and Cahill 1991). This average composition was deduced from independent measurements of 'Organic matter' from carbon by thermal optical reflectance (TOR) described in Table 4.3. This composition is consistent with earlier work by Macias et al 1981 who used  $C_4H_8O$  or 11%H, 67%C and 22%O as the average composition of their typical organic matter.

Analysis of the total hydrogen, carbon and oxygen content of filters from all 25 sites during the period January to June 1993 and removing known contributions of oxygen in 'soil' (56%), oxygen in  $(NH_4)_2SO_4$  (48%) and hydrogen in  $(NH_4)_2SO_4$  (6%) gives the best estimate of the composition of 'Organic matter' as 7%H, 85%C and 8%O. The errors on this estimate are quite large (~30%) and it is possible that carbon is systematically over-estimated and the oxygen under-estimated as discussed in the previous section. Consequently, the more recent values (Eldred et al 1990 and Eldred and Cahill 1991) of 9%H, 71%C and 20%O were used until more consistent values for the network can be obtained. Using these assumptions 'Organic matter' as calculated from hydrogen can be defined as,

$$\begin{aligned} \text{OMH} &= 11 (\text{H}-0.250*\text{S}) && \text{Aerosols in form } (\text{NH}_4)_2\text{SO}_4 && (4.8a) \\ &= 11 (\text{H}-0.156*\text{S}) && \text{Aerosols in form } \text{NH}_4\text{HSO}_4 && (4.8b) \\ &= 11 (\text{H}-0.063*\text{S}) && \text{Aerosols in form } \text{H}_2\text{SO}_4 && (4.8c) \end{aligned}$$

where the H and S concentrations were measured in  $\text{ng/m}^3$  giving the 'Organic matter' in  $\text{ng/m}^3$ . Equation (4.8a) presents 'Organic matter' for a fully neutralised aerosol, which was assumed to be most representative of the network. Equation (4.8b) is for an ammonium hydrogen sulphate aerosol and Equation (4.8c) for an acidic sulphuric acid aerosol. The average hydrogen and sulphur content for the ERDC network for 1992 were 3.5% and 5.6% of the total fine mass respectively. This gave an average 'Organic matter' content of about 23% of the fine mass for the ERDC network in 1992, if the aerosols were fully neutralised.

#### 4.3.6 Reconstructed Mass (RCM)

The sum of all the above pseudo elements and composite variables should provide a reasonable estimate of the total fine mass for comparison with the measured gravimetric mass of fine particles on our Teflon filters. To test this, the reconstructed mass (RCM) was defined as,

$$\text{RCM} = (\text{NH}_4)_2\text{SO}_4 + \text{'Salt'} + \text{'Soil'} + \text{'Smoke'} + \text{OMH} + \text{Elt.C.} \quad (4.9)$$

where the elemental carbon (Elt.C) is defined by the LIPM technique and Equation (4.4). Equation (4.9) contains contributions from all of the major elemental aerosol components measured in our fine mass except P (0.1%), V (<0.05%), Cr (<0.05%), Mn (0.1%), Co (<0.05%), Ni (<0.05%), Cu (<0.05%), Zn (0.2%), Br (0.4%) and Pb(1.2%). The sum of these excluded elements contributed on average less than 2% to the total fine particle mass during the 1992 sampling period. RCM does not include nitrates, a significant fraction of which (> 50%) were volatilised from the Teflon filter during collection, and were not measured by gravimetric mass (Eldred et al 1989). The accuracy of Equation (4.9) was tested by comparing RCM with the gravimetric weight of the filters during 1992. This is shown in Figure 4.16 where the least squares fit to the data gave  $\text{RCM} = (0.84 \pm 0.02) * \text{Weight}$  with an  $R^2 = 0.89$  across all 25 ERDC sites. This is an excellent result when one considers that the vacuum analysis reduces the fine mass by 8% on average (see above) and 2% of trace elements are not included in the definition of RCM. That leaves, on average, only 6% of the fine mass either remaining partially as nitrate or not accounted for by the reconstructed mass. It is therefore felt that

RCM as defined by Equation (4.9) is a reasonable estimate of the total fine mass on the Teflon filters.

Another definition of the reconstructed mass is the sum of all 23 elements, H, C, N, O, Na, Al, Si, P, S, Cl, K, Ca, Ti, V, Cr, Mn, Fe, Co, Cu, Ni, Zn, Br and Pb measured by IBA techniques. This sum has been named RCMS and it is not as accurate or precise as RCM defined above, since the addition of many small numbers to produce a larger number gives rise to larger errors. Furthermore, the major components of this summation the total carbon, nitrogen and oxygen concentrations assume no chemical form for these elements and they are not precisely determined by RBS techniques (see above this section). For all sites during 1992 RCMS compared with the gravimetric weight gave a value of  $(120 \pm 50)\%$ , confirming that some components of this method are overestimated. Throughout this project RCM has been used to estimate the reconstructed mass.

#### **4.4 QUALITY ASSURANCE**

Total quality assurance was addressed at all stages of the project. Extensive colour coding techniques were implemented to ensure the filter exchange processes remained simple and reliable and to ensure that there was no cross contamination of filters from different sites. Systems were introduced to keep track of each filter paper through its life cycle, from its initial weighing to its final analysis and storage for future reference. Each site was visited at least once every 3 months for a maintenance inspection and on site flow rate recalibrations of samplers. All laboratory measuring instruments were checked and calibrated before and after each use against known standards. The filters were stored in a temperature and humidity controlled room for at least 24 hours before any measurements, such as gravimetric mass, were made. Data from all the logsheets were entered into a computer which was programmed with the expected ranges for all parameters. Any filter with a parameter out of range was flagged with an error or warning code, (see below). All comments made by any of the field officers on the daily logsheets were stored on computer for cross referencing in the event of problems with a particular filter.

##### **4.4.1 Error Codes**

Each filter in the database carries with it an error code, which is a digit 0 to 9. The more significant the error the higher the number. If a filter has two or more reasons for not meeting

the zero error code condition then the highest error code is used. The type of error associated with each error code number is shown in Table 4.7.

**Table 4.7.** Errors codes that are carried with each filter analysed.

Code	Type of Error
0	No problems, all parameters within specifications
1	Warning - total fine particle mass > WHO 40 mg/m <sup>3</sup>
2	Warning - No filter vacuum gauge reading < 50 kPa
3	Warning - Magnehelic pressure drop is negative or zero
4	Warning - Flow rate less than 25% of initial value
5	Error - Volume in 24 hours is zero or less
6	Error - Mass difference on filter is negative
7	Error - Pre- or post- mass is zero
8	Error - Filter not run for 24 hrs $\pm$ 5%
9	Error - Filter torn or damaged, before or during analysis

Error codes 0-4 inclusive are warnings and do not affect the analysis or data interpretation. They are flagged in the data set to provide information that some non-critical parameters, such as a heavily loaded filter, may be outside the normal expected operating range. Errors codes 5 to 9 are errors that affect the final elemental concentration value in some way and these filters, although included in the database, should not be used in any serious analysis process as they may bias the data in unpredictable ways. For example, data with error codes from 5-9 are not used in any estimates of monthly or yearly averages for a given site. Less than 1% of all filters had error codes greater than 5 during the study period.

#### 4.4.2 Ion Chromatography (IC)

In order to check the accuracy of the IBA techniques described above 54 filters were analysed independently by ion chromatography (IC) (Maenhaut 1989). These include 4 blank filters and a selection of filters from sites 1, 2, 5, 6, 8, 10, and 13 in January and August

1992. These filters were selected to represent a range of rural and urban sites from Wollongong, Sydney and Newcastle during a typical summer and winter period.

The results of the comparison of the IBA analysis techniques with ion chromatography for sulphate ion and chloride ions are shown in Figure 4.17. If all the sulphur were present as  $\text{SO}_4^{2-}$  the PIXE sulphur concentrations should be (1/3) of the ion chromatography sulphate ion concentrations. The line of best fit to this data agrees with this hypothesis. The minimum detectable limit (MDL) for sulphate ions was about  $140 \text{ ng/m}^3$  using ion chromatography compared with the PIXE MDL of  $3 \text{ ng/m}^3$ .

Figure 4.17(b) shows that ion chromatography concentrations for  $\text{Cl}^-$  ions are higher than the PIXE concentration for elemental Cl by about 14%. The MDL for chloride ions by ion chromatography was  $90 \text{ ng/m}^3$  compared with less than  $5 \text{ ng/m}^3$  for the PIXE technique. However elemental chlorine has also been measured by neutron activation analysis NAA (see below) on a large number of filters and found to agree closely with the PIXE determination. Therefore there is greater confidence in the PIXE chlorine results than the ion chromatography chloride concentrations for assessing the total chlorine concentration. Ion chromatography results for two other ion species, nitrates and fluorides as a function of the total fine mass are shown in Figure 4.18. There are no comparable IBA techniques. A least squares fit of the ion chromatography  $\text{NO}_3^-$  concentration versus gravimetric weight gives approximately 2.2% of the total weight as nitrate but with a only  $R^2=0.425$ . As the  $\text{NO}_3^-$  concentration could be expected to be 8-15% of the total fine mass (Roberts et al 1982), these results support the idea that nitrates are readily volatilised on Teflon filters (Eldred et al 1989).

If it is assumed that the total nitrogen on a filter is composed mainly of ammonium nitrate (35%N) and ammonium sulphate (21.2%N), then as the average total nitrogen for 1992 by RBS was 5.7% of the fine mass and the average  $(\text{NH}_4)_2\text{SO}_4$  was 23% of the fine mass, we estimate the average ammonium nitrate to be 2.4% of total fine mass. This gives the nitrate ion as only 1.9% of fine mass. This is comparable with the ion chromatography estimate of 2.2% considering the larger than 30% errors for the RBS determination of nitrogen and the poor correlation between  $\text{NO}_3^-$  and total mass shown in Figure 4.18(a).

The ion chromatography fluoride results for these selected 54 filters are given in Figure 4.18(b) as a function of total fine mass. These cannot be directly compared with the PIGME total fluorine concentrations because the PIGME measurements include fluorine from the Teflon filters which overwhelms the low level fluoride concentrations shown in this figure.

Only 7 of the total of 54 filters analysed by ion chromatography showed levels of fluoride above the MDL of  $60 \text{ ng/m}^3$ . These occurred mainly in the winter time at Mayfield (ASP10, 3 readings), Warrawong (ASP8, 1 reading), Pymont (ASP2, 2 readings) and Campbelltown (ASP6, 1 reading). The highest reading of  $135 \text{ ng/m}^3$  of  $\text{F}^-$  was at Mayfield, followed by Campbelltown with  $105 \text{ ng/m}^3$  and these levels of  $\text{F}^-$  occurred for the lowest total fine particle masses. Hence it is concluded that fluorine levels are generally below  $100 \text{ ng/m}^3$  for most sites across the network.

#### 4.4.3 Neutron Activation Analysis (NAA)

As a check of the accuracy of the PIGME and PIXE analysis techniques 104 filters (including 4 blanks) were analysed independently by neutron activation analysis (NAA) for the 14 elements Na, Mg, Al, Cl, K, Ca, Ti, V, Mn, As, Br, Sr, I, and Ba. The NAA technique uses neutrons from the HIFAR reactor to activate the sample (Maenhaut 1989) and then counts the gamma rays emitted during sample decay as a means of identifying and quantifying the elements present in the sample.

The NAA technique was calibrated against a known US National Bureau of Standards reference material using 20 mg samples which was considerably below the recommended minimum sample size of 150 mg for this technique. This was done so the elemental concentrations in the standards would be comparable with those in the filters whose average mass was only 230 mg. This meant that some of the elements Ti, Ca, and As for example had poor sensitivity as the sample size was too small for this technique. As with the ion chromatography results a selection of 5 filters from each of 10 ASP sites for the months of February and July 1992 were chosen as being representative of a wide range of conditions and concentrations throughout the network. The results for all filters for all 14 elements are shown in Figure 4.19, where the PIXE/PIGME concentrations obtained from IBA techniques are plotted against the NAA concentrations over 4 decades of concentration. The line of best fit shows the two techniques agree to within 4% with a correlation coefficient of  $R^2=0.96$ . Below  $100 \text{ ng/m}^3$  most of the points on this curve lie below the line of best fit because as the concentration of an element decreases the minimum detectable limit (MDL) for the NAA technique is reached before the MDL for the IBA techniques. Nevertheless, there is good correspondence between the two techniques over the entire range of elements and concentrations. As a result there is greater confidence in the accuracy of the IBA techniques. If they are good for a range of elements covering most of the periodic table, then, as the X-ray yield is generally a smooth function of trace element atomic number (see Figure 4.3), by interpolation all elements will be reasonable.

Figure 4.20 shows the same comparison for the individual elements Mn and Cl, and again shows good agreement between the PIXE and NAA techniques. This would seem to confirm the PIXE measurements for Cl, despite them being consistently 14% lower than ion chromatography measurements for Cl (Figure 4.17(b)). Results for the elements Br, V are shown in Figure 4.21 and for Na and K in Figure 4.22. There was a good correlation between PIXE and NAA for K with  $R^2=0.99$  however the PIXE technique was consistently 24% lower than the NAA value for this element. This may be due to the poorer sensitivity and possible interelement interference (Maenhaut 1989) of NAA for this element.

No PIXE measurements were made for As, Sr, I, Ba and Mg. The NAA concentration ranges for these elements were: Mg 60 to 250  $\text{ng/m}^3$ , As 1 to 10  $\text{ng/m}^3$ , Sr less than 60  $\text{ng/m}^3$ , Ba less than 30  $\text{ng/m}^3$  and I 1 to 10  $\text{ng/m}^3$ . Arsenic is a trace element generally associated with coal combustion but the PIXE technique cannot measure the element As in the presence of larger amounts of Pb. The NAA measurements show that the average As levels across the ASP network are less than 1  $\text{ng/m}^3$ , with maximum levels of between 3 and 9  $\text{ng/m}^3$  (Pymont, July 1992). Levels of around 3  $\text{ng/m}^3$  were measured at Campbelltown and Badgerys Creek in July 1992.

## 5. RESULTS AND DATA INTERPRETATION

### 5.1 THE ERDC PROJECT DATABASE

Information about the chemical composition of particles collected on the filters are stored in a chemical database. Each filter is assigned a unique code which contains the information about the site location and date of collection. This code is followed by sampling and quality assurance information, and all data for the measured concentrations of each element and ion. The data are sorted first by site number into 25 major divisions (corresponding to the 25 sampling sites) and then by date, to facilitate computer scanning and data retrieval. A simplified diagram of the chemical database is shown in Figure 5.1. The data described in this report covers the period January 1992 - June 1993. Table 5.1 lists the fine particle concentrations that are measured and stored in the chemical data base.

**Table 5.1** Species measured and stored in the chemical data base

mass	sodium	potassium	nickel	chloride ions
elemental carbon	aluminium	calcium	chlorine	bromide ions
hydrogen	silicon	titanium	zinc	nitrate ions
carbon*	iron	vanadium	bromine	sulphate ions
nitrogen*	phosphorus	chromium	lead	copper
oxygen*	sulfur	manganese	fluoride ions	cobalt

\* data for these elements are only available for the period January - June, 1993. The chemical database (January 1992 - June 1993) currently contains results for 150,000 chemical measurements from nearly 5,000 filters.

The chemical database is designed to be linked to a meteorological database containing hourly average values of wind speed and direction, and daily totals of rainfall. Unlike the chemical database which holds data for only Wednesday and Sunday, the meteorological database has been designed to hold data from every day of the year. An effort is being made to obtain meteorological data at or close to 20 of the 25 sampling sites so that the interpretation of pollution events can be improved.

Data from the project is stored in ASCII format for use on mainframe and IBM computers, and in Microsoft Foxbase file for use on Macintosh computers. Programs have been written in Foxbase to allow presentation of combined chemical and meteorological results for any filter and for the production of blocks of data for importation into spreadsheet programs. Microsoft EXCEL, both IBM and Macintosh versions, was the spreadsheet program chosen

for the study. To overcome problems of large files and memory requirements associated with the use of EXCEL, data blocks were limited to a maximum period of six months. To produce spatial plots of data the MacGridzo (Macintosh computers) and GeoEAS (IBM computers) packages were used.

## **5.2 METHODS OF DATA ANALYSIS AND PRESENTATION**

The data from the ERDC project may be analysed at three different levels, by filter, site and region:

### **5.2.1 Analysis of filter**

It is possible to look at the ratios of elements for individual filters and infer particular sources of particles are contributing to the fine particle mass measured at a particular site. For example a ratio of lead to bromine of approximately 2:1 infers the presence of particles from the combustion of leaded petrol, while high ratios of copper, lead and zinc to other metals indicate industrial smelting of sulphide ores; and a high ratio of potassium to iron may indicate 'smoke' from combustion of wood.

### **5.2.2 Elemental composition of filters by site**

Measurements of elements and ions at a site can be plotted against the day of the year so that day-to-day variability and variations from season to season are apparent. Typical values and anomalies are easily detected from plots of this type. For example, the high concentrations of total mass, hydrogen, carbon and potassium at Wilton on 23rd August 1992 (Figure 5.2) may be linked to a bush fire 20 km to the west.

Data from a particular site can be used to obtain average values for the ratios of different elements. For example, correlations between lead and bromine, for instance, are high at urban sites such as Rozelle when all the data for a six-month period are averaged (Figure 5.3). The same is true for sodium and chlorine from sea 'salt' at coastal sites, as shown in Figure 5.4 for Cape Grim in Tasmania.

### 5.2.3 Elemental composition by region

On days of particular interest, such as high pollution days, it is useful to examine the distribution of particular pollutants throughout the region. Data may be presented either as a histogram (eg for mass; Figure 5.5) or as a spatial plot over the region.

Sites in a region can be ranked in terms of annual or monthly average concentrations of species, (eg. Table 5.5). Values of elements averaged over extended periods are less subject to random fluctuations than daily values and are better indicators of seasonal trends. Data may be presented as either a histogram (eg. lead; Figure 5.6) or as a spatial plot showing the variations in concentration over the region (eg. lead; Figure 5.7). Spatial plots are helpful for visualising the areas with high and low pollutant levels; values can be related to meteorological conditions, source characteristics and atmospheric chemistry.

An alternative way of displaying regional variation in the species being measured is to divide the study region into sectors based on a parameter such as the distance from Sydney or the degree of urbanisation. This shows that certain sectors, eg. those situated long distances from urban centres, have lower concentrations of many airborne pollutants (eg. fine mass; Figure 5.8) than those in urban centres.

## 5.3 DISCUSSION OF RESULTS

The main body of results for the period January 1992 - June 1993 is given in two appendices at the end of this volume. Appendix 1 is in three volumes and contains daily concentrations of elements at each site. Appendix 2 contains the monthly average concentrations of elements at each site

The first appendix gives the daily average data for the chemical composition of particles at all 25 sites. Data are presented as histograms, plotting daily concentrations against date in six-month blocks (Jan-Jun 92, Jul-Dec 92, Jan-Jun 93), a volume for each block. These plots allow the daily variations at each site to be readily observed. The second appendix gives the average monthly concentration for each element at each site. Data are presented as histograms, plotting average monthly concentration against site number in six month blocks (Jan-Jun 92, Jul-Dec 92, Jan-Jun 93). These plots allow the sites to be compared.

The discussion of results in this volume draws heavily on Appendices 1 and 2, and also includes material from interpretive studies which have analysed the data in other ways.

### 5.3.1 Annual average concentrations of elements

The average concentrations of elements in the air collected at all sites of the network during 1992 are given in Table 5.2, the average conditions under which the filters were collected are given in Table 5.3 and the average elemental composition of the particles collected on the filters is given in Table 5.4.

**Table 5.2.** Average concentrations of elements and pseudoelements in the air collected at all sites in the network throughout 1992. Standard deviations are also given.

Element	Concentration (ng/m <sup>3</sup> )	Element	Concentration (ng/m <sup>3</sup> )
H	270±150	V	0.4±0.5
Na	210±250	Cr	0.5±0.4
Al	33±29	Mn	6±22
Si	58±37	Fe	71±140
P	7±3	Co	0.5±0.6
S	430±190	Ni	0.5±0.7
Cl	270±280	Cu	2±3
K	52±42	Zn	17±27
Ca	25±24	Br	33±55
Ti	3±3	Pb	88±122

Pseudoelement	Concentration (ng/m <sup>3</sup> )	Pseudoelement	Concentration (ng/m <sup>3</sup> )
'soot'	1700±1500	(NH <sub>4</sub> ) <sub>2</sub> SO <sub>4</sub> *	1800±770
'soil'	430±460	'smoke'	9±58
sea 'salt'	530±620	'organic matter'	1800±1600

\* Not corrected for seawater sulphate (~5% of total)

SECTION 5 - RESULTS AND DATA INTERPRETATION

**Table 5.3.** Average conditions under which filters were collected. Standard deviations for the 25 sites are also given.

Parameter	Units	Value
Air flow rate	L min <sup>-1</sup>	22±1
Air volume sampled	m <sup>3</sup>	32±2
Maximum temperature	°C	29±6
Minimum temperature	°C	8±6
Mass of particles on filter	µg	240±107
Thickness of Teflon filter	µg cm <sup>-2</sup>	224±19
Coefficient of absorption (b <sub>ap</sub> )	µm <sup>-1</sup>	17±15

**Table 5.4.** Average elemental composition of particles collected on the filters at all sites in the network throughout 1992, expressed as a percentage of the total fine particle mass.

Element	Abundance (%)	Element	Abundance (%)
H	3.5	Ti	0.04
Elit.C <sup>1</sup>	23	V	0.01
N <sup>2</sup>	6	Cr	0.01
Na	2.8	Mn	0.08
Al	0.4	Fe	0.9
Si	0.8	Co	0.01
P	0.09	Ni	0.01
S	5.6	Cu	0.03
Cl	3.5	Zn	0.2
K	0.7	Br	0.4
Ca	0.3	Pb	1.2

<sup>1</sup> Estimated by LIPM as 'soot'.

<sup>2</sup> Data from RBS; available only from 1/1/93; value is approximate only (±50%).

The average concentration of fine particle mass was  $7.7 \mu\text{g}/\text{m}^3$  for the whole network (standard deviation =  $4.0 \mu\text{g}/\text{m}^3$ ). Elemental carbon ('soot') was the most abundant element in the fine particles, followed by sulphur (largely from fuel burning), nitrogen (in ammonium and nitrate ions), sodium and chlorine (largely present as sea salt) and hydrogen (from organic matter).

The fine particles collected from the entire network had an average composition of 23% 'organic matter', 23% 'ammonium sulphate', 22% 'soot', 7% sea 'salt', 6% 'soil', 1% lead with the remainder being trace elements, residual water and other inorganic ions such as nitrate. The pseudoelements account for 81% of the fine mass of material collected on the filters. It is known that approximately 8-10% water is lost from the filters when they are placed in an evacuated chamber during ion beam analysis, and approximately 5% by weight of nitrate ions were found in typical filters analysed by ion chromatography. This means that approximately 95% of the total mass is explained. If the degree of neutralisation of sulphuric acid aerosols by ammonia is only 50%, the percentage by weight of ammonium hydrogen sulphate is 20% and about 92% of the total mass is explained.

Particles of 'soot', 'soil', 'ammonium sulphate', 'organic matter' and lead, which are typical of fuel combustion processes, comprise around three-quarters of the mass of the fine airborne particles. This indicates the importance of combustion sources for this particle-size fraction. Many of the elements listed in Table 5.2 have local sources within the study area and are strongly influenced by meteorological factors, leading to widely different concentrations at the sampling sites; this is reflected in the large standard deviations for many of the elements.

The sampling sites may be ranked in terms of the concentrations of major components as shown in Table 5.5 where the ranking of the 25 network sites for several fine particle components are listed.

### 5.3.2 Fine particle concentrations in the ASP study sectors

The monthly average concentrations of major aerosol components at the different sites of the network are given in Appendix 2. To facilitate analysis of data, the study area was divided into sectors 0, 0-25, 25-50, 50-100 and 100-200 km from the Sydney Central Business District (SCBD) with additional sectors for the Wollongong and the Newcastle city areas (Table 5.6); Cape Grim in Tasmania was treated as a separate sector. To date, there has been no evaluation of meteorological conditions associated with the occurrence of

SECTION 5 - RESULTS AND DATA INTERPRETATION

different elements measured at each site in the network. However, there generally a higher frequency of onshore winds during the warmer months of the year, while during the cooler months the prevailing synoptic winds are westerly to south westerly. Cold air drainage flows and nocturnal radiation inversions, which may inhibit the dispersion of fine particles, are more frequent in the winter months.

**Table 5.5.** Ranking of sites in terms of the concentrations of major aerosol components and indicator elements. Values are average concentrations recorded during 1992 in ng/m<sup>3</sup> and numbers are only expressed to three significant figures.

Total mass	'Ammonium sulphate**	'Organic matter'	'Soil'	'Soot'
Mayfield 12200	Warrawong 2680	CullBullen 3620	Mayfield 1610	Mascot 4210
Pymont 11600	Pymont 2360	Mascot 3060	Pymont 1060	Pymont 3940
Mascot 10800	Muswbrk 2350	Rozelle 2990	Warrawong 1020	Mayfield 3790
Rozelle 10600	Mayfield 2300	Pymont 2890	Mascot 672	Lidcombe 3020
Lidcombe 10000	Rozelle 2150	Lidcombe 2560	Richmond 581	Rozelle 2980
Warrawong 9840	Lidcombe 2050	Mayfield 2340	Lidcombe 537	CullBullen 2780
CullBullen 9740	Mascot 1960	Richmond 2220	Rozelle 493	Warrawong 2320
Campbtwn 8950	Bellambi 1930	Badgery Ck 2150	Putty 472	Mac. Uni. 2160
Bellambi 8590	Campbtwn 1920	Mac. Uni. 2150	Doyalson 393	Campbtwn 2020
Mac. Uni. 8550	Albion Pk 1860	Campbtwn 1960	Muswbrk 375	Richmond 1530
Moss Vale 8350	Mac. Uni. 1820	Moss Vale 1880	Tomago 346	Doyalson 1310
Richmond 7250	Wilton 1790	Bellambi 1730	Mac. Uni. 340	Muswbrk 1300
Badgery Ck 7040	Lucas Hts 1730	Blkheath 1590	Campbtwn 327	Moss Vale 1270
Lucas Hts 6860	Tomago 1690	Putty 1500	Bellambi 275	Lucas Hts 1220
Muswbrk 6480	Badgery Ck 1620	Doyalson 1400	CullBullen 272	Bellambi 1190
Cape Grim 6460	CullBullen 1610	Warrawong 1320	Albion Pk 255	Badgry Ck 1180
Wilton 6410	Oberon 1460	Wilton 1290	Badgry Ck 242	Wilton 1160
Tomago 6150	Putty 1460	Muswbrk 1210	Lucas Hts 240	Tomago 1030
Doyalson 6058	Richmond 1420	Tomago 1150	Mudgee 232	Albion Pk 969
Albion Pk 5950	Mudgee 1420	Lucas Hts 962	Moss Vale 196	Blkheath 816
Blkheath 5730	Blkheath 1410	Mudgee 915	Wilton 189	Putty 645
Putty 5360	Moss Vale 1370	Oberon 882	Oberon 147	Mudgee 567
Mudgee 4580	Doyalson 1360	Albion Pk 843	Crookwell 134	Oberon 455
Oberon 4120	Crookwell 1070	Crookwell 793	Blkheath 130	Crookwell 348
Crookwell 3460	Cape Grim 985	Cape Grim 417	Cape Grim 96	Cape Grim 342

SECTION 5 - RESULTS AND DATA INTERPRETATION

**Table 5.5 (cont)** Ranking of sites in terms of the concentrations of major aerosol components and indicator elements. Values are average concentrations recorded during 1992 in ng/m<sup>3</sup> and numbers are only expressed to three significant figures.

	Sea 'salt'	Potassium	Iron	Zinc	Lead
Cape Grim	2160	Mayfield 141	Mayfield 431	Pymont 75	Mascot 334
Bellambi	1750	Warrawong 131	Warrawong 281	Mayfield 73	Pymont 297
Warrawong	994	Pymont 66	Pymont 270	Lidcombe 40	Lidcombe 240
Pymont	797	Rozelle 66	Mascot 105	Warrawong 36	Rozelle 239
Mayfield	784	Mascot 65	Lidcombe 66	Mascot 35	Mac. Uni. 133
Lidcombe	660	Lidcombe 62	Rozelle 57	Rozelle 32	Campbtwn 132
<b>Rozelle</b>	657	Albion Pk 60	Tomago 46	Mac. Uni. 19	Mayfield 121
Tomago	629	Bellambi 60	Albion Pk 46	Tomago 17	Warrawong 105
Mascot	604	Mac. Uni. 58	Bellambi 45	Bellambi 11	Lucas Hts 81
Lucas Hts	598	Richmond 55	Richmond 40	Albion Pk 11	Richmond 79
Albion Pk	565	Tomago 48	Mac. Uni. 40	Lucas Hts 10	Badgry Ck 60
<b>Doyalson</b>	512	Campbtwn 46	Putty 39	Campbtwn 9	Bellambi 52
Mac. Uni.	488	Doyalson 43	Campbtwn 36	Richmond 9	Doyalson 51
Campbtwn	426	Badgry Ck 42	Doyalson 33	<b>Doyalson</b> 9	Albion Pk 43
Wilton	414	Lucas Hts 39	Lucas Hts 28	Badgry Ck 8	Wilton 43
Badgry Ck	372	CullBullen 38	Badgry Ck 24	Wilton 6	Moss Vale 34
Muswbrk	260	Wilton 36	Muswbrk 22	CullBullen 5	Tomago 29
Richmond	259	Cape Grim 35	Wilton 21	Muswbrk 4	CullBullen 25
<b>Putty</b>	209	Putty 33	Moss Vale 17	Moss Vale 4	Muswbrk 12
Moss Vale	158	Moss Vale 31	Mudgee 14	Putty 2	Mudgee 8
<b>Blkheath</b>	150	Muswbrk 30	CullBullen 13	Mudgee 2	Blkheath 7
CullBullen	147	Mudgee 27	Blkheath 10	Blkheath 2	Putty 7
<b>Mudgee</b>	144	Oberon 20	Oberon 10	Oberon 2	Oberon 5
Oberon	98	Blkheath 20	Crookwell 8	<b>Crookwell</b> 1	Crookwell 2
Crookwell	82	Crookwell 15	Cape Grim 3	Cape Grim 0	Cape Grim 1

\* Assuming all sulphate is fully neutralised as ammonium sulphate.

Not corrected for seawater sulphate. The average sea-salt correction was 5% (range 1 to 15%).

**Table 5.6.** Sampling sites allocated to the sectors 0, 0-25, 25-50, 50-100, 100-200, km from the Sydney Central Business District (SCBD), and to the Wollongong and Newcastle sectors. Cape Grim (Tasmania) is a global baseline monitoring station.

Sector	Sites
SCBD	2,3
0-25 km	5,17,23
25-50 km	1,6,18,21
50-100 km	12,14,24
100-200 km	4,13,15,16,19,20,22
Wollongong	7,8,9
Newcastle	10,11
Cape Grim	25

#### 5.3.2.1 Sydney CBD sector: (*Pymont and Rozelle*)

Winter maxima in mass, 'organic matter', 'soil', carbon, iron, zinc, potassium and lead are apparent. This is probably due to the poorer ventilation of the area during winter and the abundance of particle sources in the vicinity. Increased domestic combustion of fossil fuels may also contribute. Sea 'salt' concentrations were lowest during winter due to the rarity of winds with easterly components (especially north easterlies). 'Ammonium sulphate' concentrations varied little during the year; the enhanced conversion of sulphur dioxide to sulphate species in summer may be offset by the better ventilation of the area during this time of the year. Alternatively, the emission of sulphate from motor vehicles, particularly diesel vehicles may be uniform throughout the year.

The Pymont site rated in the top four sites for each of the ten major aerosol components. Most components (mass, 'organic matter', 'soil', carbon, potassium, iron, zinc and lead) were found at higher concentrations during the winter than the summer months. The power station and flour mill surrounding the site were demolished during the later months of the sampling period in the middle of 1993 and this may have influenced the quantity and types of fine particles collected during this period. The Rozelle site showed a similar profile to Pymont, but with lower concentrations of 'ammonium sulphate', 'soil', 'soot', sea 'salt', iron and zinc.

**5.3.3.2 0-25 km sector, (*Lidcombe, Macquarie University and Mascot*):**

Patterns in this sector were the same as those for the Sydney CBD sector. The concentrations of airborne species were also similar. The Lidcombe site in central Sydney was one of the top five (with respect to PM<sub>2.5</sub>), most heavily polluted sites in the study. Macquarie University, situated north of the urban and industrialised areas of Sydney adjacent to the Parramatta River valley, generally recorded lower concentrations than the inner-city sites. Concentrations at Mascot were similar to those at Pymont, Rozelle and Lidcombe.

**5.3.3.2 25-50 km sector (*Lucas Heights, Campbelltown, Richmond and Badgerys Creek*):**

Patterns in this sector were again similar, except there was not a winter maxima for mass, zinc and iron, and there was a winter minimum in 'ammonium sulphate' concentrations, which may be linked to changes in meteorology. Salt concentrations decreased as distance from the coast increased.

The Lucas Heights site, on the southern edge of Sydney, can under suitable meteorological conditions, be subject to particle pollution from central Sydney or locally from the Menai tip. The mass of fine particles was highest during summer, especially February. Concentrations of 'organic matter', 'soil', 'soot', potassium and lead were highest during winter. Iron and zinc were also more abundant during winter than summer, but had maxima in March.

Campbelltown, southwest of Sydney, receives pollution from Sydney under north easterly wind flow, especially during summer. A summer maximum in 'ammonium sulphate' concentration was observed and winter maxima for 'organic matter', 'soil', 'soot', potassium and lead. Under certain conditions lead from motor vehicles at this site was comparable or higher than some inner city sites such as Rozelle and Mascot.

Richmond lies in the north west section of the Hawkesbury River valley in the west of the Sydney region. Concentrations of mass, 'organic matter', 'soot', zinc, lead and potassium were highest in winter, most probably due to poorer dispersion in the region during this period; local combustion sources may be significant contributors in winter. Badgerys Creek, on the western outskirts of Sydney showed seasonal variations in component concentrations similar to those of the other Sydney sites.

**5.3.3.3 50-100 km sector, (*Blackheath, Wilton and Doyalson*):**

Patterns were similar to those of the 25-50 km sector, except that winter minima appeared for 'soil' and iron. The winter minimum for 'ammonium sulphate' was more marked. At Blackheath, west of Sydney and adjacent to the Blue Mountains National Park, 'Ammonium sulphate', 'soil' and iron concentrations were lowest during winter. 'Organic matter', 'soot' and potassium were highest during winter, possibly due to domestic combustion of wood. Sea 'salt' concentrations at Blackheath were amongst the lowest recorded in the study, due to the long distance between the site and the coast, and lead concentrations were low. Possible sources of particles at this site include the Sydney urban area (under strong easterly components winds) and the power stations at Wallerawang and Mount Piper to the west.

Wilton, under suitable wind conditions, may receive particles from sources in either Sydney or Wollongong. Concentrations of 'Ammonium sulphate', sea 'salt' and iron were lowest during winter; other species showed complex monthly variations.

Doyalson, south of the power stations of Eraring and Vales Point, and in the grounds of the Munmorah power station, recorded one of the lowest 'Ammonium sulphate' concentrations. This requires meteorological investigation. Carbon and lead recorded winter maxima, but other species exhibited complex behaviour.

**5.3.3.4 100-200km sector, (*Muswellbrook, Oberon, Mudgee, Putty, Moss Vale, Crookwell and Cullen Bullen*):**

Patterns were similar to those for the 50-100 km sector except that mass was highest during the early months and declined steadily through the year. Concentrations of most particle species were lower in this sector than in the central Sydney region by approximately the following factors: mass (3), 'ammonium sulphate' (3), organics (4), 'soil' (10), 'soot' (8), sea 'salt' (10), potassium (7), zinc (35) and lead (30).

Muswellbrook, at the northern extremity of the study area, near Liddell and Bayswater power stations, is downwind from Newcastle under conditions of south easterly wind flow. 'Ammonium sulphate', 'soil', and iron recorded higher concentrations during the summer than the winter months, possibly linked with wind direction. 'Organic matter', potassium, zinc and

lead showed strong maxima during winter, possibly due to local combustion of wood, coal and petrol, coupled with poorer ventilation in winter.

Both Oberon and Mudgee exhibited winter minima in concentrations of 'ammonium sulphate', 'soil' and iron. Oberon also showed winter minima in concentrations of 'soot', zinc and lead. Sea 'salt' concentrations were low due to the long distance from the coast. Oberon showed one of the lowest PM2.5 levels in the study. Mudgee, at the north west corner of the study area, was amongst the lowest five sites in terms of annual concentrations of fine mass, 'organic matter', 'soot', sea 'salt', potassium and zinc.

Putty, 100 km inland from Newcastle, lies between a power generating regions to the north and south west, and is north west of Sydney. Under suitable wind conditions, it may receive particles from any of these sources, meteorological data are required to test this hypothesis further. 'Ammonium sulphate', sea 'salt', zinc and lead at this site showed winter minima. Other elements exhibited more complex behaviour.

The Sydney region, (under north to north easterly wind flow), and Wollongong, (under easterly flow) are possible source regions for particles measured at Moss Vale. This site recorded the fourth lowest concentrations of 'ammonium sulphate', with a minimum in the winter. 'Organic matter', 'soil', 'soot', iron, zinc, lead and potassium recorded winter maxima.

Crookwell, approximately 200 km southwest of Sydney, showed one of the lowest PM2.5 levels of the study. 'Ammonium sulphate', 'organic matter', 'soil', 'soot', iron, zinc, lead and potassium displayed winter minima.

Cullen Bullen lies in a valley 30 km north west of Wallerawang Power Station and 120 km north west of Sydney. Mass, 'organic matter', 'soot', zinc, lead and potassium showed strong winter maxima. The concentration of 'organic matter' (as an annual average) was the highest recorded at any site in the study area. This is probably due to the domestic combustion of coal during winter [observed during site visits], combined with the poor ventilation of the area. 'Ammonium sulphate' was at minimum concentration during winter. Sea 'salt' concentrations were amongst the lowest recorded.

**5.3.3.5 Wollongong sector, (*Albion Park, Warrawong and Bellambi Point*):**

Concentrations of species in airborne particles were generally lower than in the Sydney CBD or 0-25 km sector. The monthly values of mass, 'ammonium sulphate', 'soil', carbon, sea 'salt', iron, zinc and potassium exhibited winter minima. Concentrations of organics and lead did not follow this pattern, probably due to the presence of local sources.

Albion Park is a receptor region for airborne particles from Wollongong-Port Kembla industrial area under north-east wind flow, especially during summer. This may explain the January-February maxima for 'ammonium sulphate', sea 'salt' iron, zinc and potassium. 'Organic compounds' were most abundant during winter and may have been due to local combustion sources. 'Soot' concentrations were similar throughout the year;

Warrawong, near the steelworks and copper smelter at Port Kembla, showed one of the highest levels of PM<sub>2.5</sub> of the study, recording annual average concentrations of 'ammonium sulphate', potassium, iron and zinc which placed it amongst the top four sites. 'Ammonium sulphate' levels were the highest of all the sites. Sea 'salt' concentrations were also high, probably due to the proximity of the site to the coast. Winter minima were recorded for all species except 'organic compounds' (mass, 'ammonium sulphate', 'soil', 'soot', sea 'salt', iron, zinc, lead and potassium).

The coastal site of Bellambi Point is a receptor for particles from Wollongong,(under southerly wind flow), and from Sydney (under north to north-easterly wind flow). Some species (mass, 'ammonium sulphate', sea 'salt', iron) display winter minima, but the monthly behaviour of other species was complex. Sea 'salt' concentrations were the second highest of all the sites in the study, probably due to the close proximity of the coast.

**5.3.3.6 Newcastle sector, (*Mayfield, Tomago*):**

Concentrations of species were generally similar to those in the Sydney CBD and 0-25 km sector, except that lead and 'organic matter' were higher in the Sydney area. The monthly values of 'ammonium sulphate', 'soil', sea 'salt', potassium and iron showed winter minima; while concentrations of organic matter', 'soot' and lead had winter maxima; and concentrations of mass and zinc showed little monthly variation.

Mayfield was one of the sites recording the highest levels of PM<sub>2.5</sub>, with the highest concentrations of mass, 'soil', potassium and iron, and being amongst the top five for 'ammonium sulphate', 'soot' and zinc. 'Ammonium sulphate', 'soil', sea 'salt', iron and potassium exhibited winter minima. Concentrations of lead, 'soot' and 'organic matter' exhibited winter maxima. Mass remained remarkably constant throughout the year. Tomago is a receptor of particles from sources in Newcastle under southerly wind flow. Concentrations of 'organic matter' and carbon showed winter maxima, while mass, 'soil', iron, zinc and lead showed autumn maxima. Sea 'salt' concentrations were lowest during winter.

#### 5.3.3.7 Tasmania, (*Cape Grim*):

Cape Grim is a global baseline station for monitoring atmospheric composition. [Note that the data provided are for the period July 1992 to June 1993.] It recorded the lowest levels of all species of anthropogenic origin, and concentrations were approximately constant throughout the year. Only 'ammonium sulphate' showed a significant seasonal trend, with values December-May being generally higher than those during the remainder of the year. This may reflect a change in the balance between oceanic and continental input or seasonal changes in oceanic production of dimethylsulphide (Gibson et al., 1994).

### 5.3.3 Seasonal variations

Particle species derived from fossil fuel combustion (eg. 'soot', 'organic matter', 'soil', potassium and lead) were generally found in the atmosphere at highest concentrations during winter. The notable exception to this generalisation was 'ammonium sulphate', which was usually found at lower concentrations during winter. At the inner Sydney sites, 'ammonium sulphate' concentrations remained similar during winter and summer.

Sea 'salt' concentrations were lowest during winter at all NSW sites, possibly associated with the reduced frequency of winds with easterly components during winter. At Cape Grim, sea 'salt' concentrations remained constant.

The variation in composition of the fine aerosol particles with season is illustrated in Figure 5.8 for typical sites in Sydney (Rozelle), Newcastle (Mayfield), Wollongong (Warrawong) and a rural area (Crookwell). In the three urban areas, the proportions of elemental carbon ('soot') and 'organic matter' are greater in the winter than the summer, while 'ammonium sulphate'

and 'salt' concentrations are lower. At Crookwell, a winter decrease is observed in 'ammonium sulphate' and 'soil'; sea 'salt', 'organic carbon' and 'soot' remain similar in concentration during the two seasons.

#### **5.3.4 Urban, non-urban and rural differences**

Urban areas generally recorded higher concentrations of particle species associated with human activities with lower concentrations being measured in rural areas. Fine particles may be carried long distances and hence contribute to particle levels in areas well removed from their source, (eg. 'Ammonium sulphate', 'organic matter', 'soil', 'soot', potassium, iron and zinc). Lead concentrations decline rapidly with distance from urban areas. Sea 'salt' declines rapidly with distance from the coast, independently of urban or industrial sources. Mass is generally highest in urban areas, but may also be high in non-urban areas possibly due to the contribution of local sources. There were a number of surprises: Cullen Bullen had the highest concentration of 'organic matter' of any site in the study, presumably due to a large winter consumption of coal for domestic heating and local meteorological factors. The very different seasonal behaviour of pollutant concentrations at many sites requires geographical, meteorological and statistical interpretation.

### **5.4 DISCUSSION OF FINE PARTICLE COMPONENTS**

#### **5.4.1 Total fine particle mass**

'Soil', 'soot', organics and 'ammonium sulphate' are major contributors to the total mass. The average concentrations of fine particle mass in all sectors and at all sites in the network during 1992 are given in Figures 5.9. Figure 5.10 shows the concentrations at all sites for June and December 1992. Greatest concentrations were found in industrial and urban areas, with Mayfield and Pymont having the highest values. Rural areas (for example Crookwell, Oberon) generally had much lower concentrations, the exception being Cullen Bullen where extensive domestic coal burning was observed to occur during the winter.

Other methods of collecting airborne particles include the measurement of total suspended particles (TSP) which measures particles of diameters 2.5 - 50  $\mu\text{m}$ . In the study area there were two sites both PM2.5 and TSP were measured, namely Mayfield and Rozelle. At these sites, TSP were measured on a six-day cycle and PM2.5 samples were obtained every

Wednesday and Sunday. As a result, greater variation may be expected in the results than if the data were collected on the same days. The ratio (TSP/PM<sub>2.5</sub>) for lead and iron for one-month periods of 1992 are plotted in Figure 5.11 and 5.12 for Mayfield and Rozelle, respectively, where data are available. The average annual values of these ratios are given in Table 5.7 together with some data for Warrawong. These measurements demonstrate that TSP is a poor indicator of PM<sub>2.5</sub> particles, and vice versa. For lead, there is no significant difference between the average annual ratios at Mayfield, Warrawong and Rozelle, showing similar particle size distributions at each sites.

**Table 5.7.** Annual average ratios of (TSP/PM<sub>2.5</sub>), for Pb and Fe during 1992 at Mayfield Rozelle and Warrawong. Standard deviations are given after each value.

Site	TSP / PM <sub>2.5</sub>	(TSP/ PM <sub>2.5</sub> ) for Pb	(TSP/ PM <sub>2.5</sub> ) for Fe
Mayfield <sup>1</sup>	7.0±2.7	2.0±0.7	27±11
Rozelle <sup>2</sup>	4.1±1.6	1.8±0.9	
Warrawong <sup>2</sup>	5.6±2.2	1.9±0.7	

<sup>1</sup> TSP data provided by BHP, Newcastle.

<sup>2</sup> TSP data provided by NSW EPA.

#### 5.4.2 'Soil'

Mayfield recorded the highest annual windblown 'soil' concentration. Given its siting, the contribution from industrial combustion processes would be expected to be important (since iron and potassium were also high). Urban and industrial sites recorded the highest values.

Plots of 'soil' against its constituents (silicon, aluminium, titanium calcium and iron) are generally linear, with correlation coefficients close to unity. In the case of Oberon during the period January to June 1992, this is true for all elements (Figure 5.13). When 'soil' is plotted against silicon for all sites (Figure 5.14(a)), a line of minimum slope may be drawn which may be representative of background silicon conditions in the study area. Points lying well above the line contain excess soil components. At the Mayfield site (Figure 5.14(b)), a large proportion of filters contain soil components with concentrations above this natural level.

### 5.4.3 Sulphur

Concentrations of sulphur in fine particles are generally lower in winter than in summer, as shown by the monthly averages for all sites in the last plot of Figure 5.15. The overall trend is apparent at Wollongong and Newcastle sites, and at sites further than 25 km from the centre of Sydney. At sites near the centre of Sydney, there is little difference between winter and summer values. This phenomenon requires further investigation in conjunction with meteorological data.

Diesel fuel burnt in the Sydney city area contains approximately 2% sulphur and may be another source of fine particle sulphate at some locations. Sea 'salt' particles contain a small proportion of sulphur (mass ratio, S/Na = 0.084). To account for this contribution average values should be reduced by about 4%. Unless indicated, this correction has not been made and values of total sulphur are given in this report.

Spatial plots of sulphate concentrations (eg. Figure 5.16) demonstrate that the highest values are found around the urban/industrial areas of Newcastle-Sydney-Wollongong and in the upper Hunter valley (Muswellbrook). In summer, the highest values were at the far north and south of the study area. Power stations and industrial sources are the main emitters of sulphur in the region. During winter, highest concentrations of sulphur were found in particles collected from the central Sydney area.

Relatively high levels of sulphur were found at some sites during days of high photochemical pollution during the summer, eg. 27th December (Figure 5.17). Sites at Wilton, Badgerys Creek, Campbelltown, Muswellbrook and Lucas Heights were found to have sulphur levels as high or higher than those in the inner Sydney region.

### 5.4.4 Lead

The average concentration of fine particle lead (<2.5  $\mu\text{m}$ ) over the whole network for the 12 months of 1992 was 83  $\text{ng}/\text{m}^3$  with a mean monthly winter value of 123  $\text{ng}/\text{m}^3$  and a mean monthly summer value of 55  $\text{ng}/\text{m}^3$ . Weekend (Sunday) and weekday (Wednesday) values were not significantly different. The highest 24-hour average concentration for the whole network was recorded at Lidcombe on 12 July 1992 (1700  $\text{ng}/\text{m}^3$ ). Lead accounted for 0.2 to 2.5% of the particle mass collected on the filters. These results are consistent with those obtained by McKenzie and Newton (1978) in a two month study of lead in airborne fine

## SECTION 5 - RESULTS AND DATA INTERPRETATION

particles at five sites in Sydney, despite the large changes in Pb sources over that time, particularly the reduction of Pb in petrol.

Typical results for lead concentrations at an urban site (Mascot) and a rural site (Oberon) are given in Figure 5.18 for each sampling day during the year. Winter lead levels were significantly higher than summer levels at Mascot, the maximum occurring in June-July. The lead data for Oberon is a factor of 60 less than for the Mascot site, reflecting the much lower lead levels encountered in rural areas. There is no seasonal trend in the Oberon data.

Average and maximum lead values recorded during 1992 for each of the sectors (Table 5.6) are shown in Figure 5.19. There is a 30 fold decline in lead concentrations between the Sydney central business district and the 200 km sector. Fine particle lead is associated with emissions from motor vehicles and changes in lead concentrations are consistent with differences in motor vehicle density between sectors. In 1991, there were about 2400 registered vehicles per square km in the 0 km sector, 1400 in the 25 km sector and less than 100 in the 50 km sector (based on data obtained from the Roads and Traffic Authority for numbers of registered vehicles in different postcode areas).

Despite the presence of heavy industry in the Wollongong and Newcastle sectors, the fine particle lead levels recorded are lower than those found within a 100 km radius of Sydney. Average monthly lead levels were calculated for each sector (Figure 5.20). A winter maximum is apparent in all sectors except Wollongong. The winter maximum is most obvious in the inner Sydney area, where lead concentrations are a factor of 7 higher in the winter than in the summer months. The maximum becomes less pronounced with distance from the city, reducing to a factor of only 2 in the more distant sectors.

The levels of airborne lead at the different sampling sites on a high pollution day (14 June) are shown in Figure 5.21. The concentrations of lead are hundreds of times less in the rural areas than in the inner Sydney area. Again, the Newcastle and Wollongong sites have lower levels of fine particle lead than the inner Sydney sites.

The lead present in fine particles (<2.5  $\mu\text{m}$  equivalent aerodynamic diameter) represents only a part of the total airborne lead. Total airborne lead is measured by analysis of lead in total suspended particulates (TSP). Significant quantities of lead may occur in such particles around industrial sites which produce particles by mechanical means or where coagulation is important. Data for lead in TSP were available at two sites used by the ASP study (Rozelle and Mayfield). A comparison of TSP and fine particle lead at these sites is given in Figure 5.22. Fine particle lead accounts for approximately 50% of the TSP lead at each site. During

summer, the percentage is lower (30-50%), while in winter it is higher (50-100%). It is likely that automobile exhausts represent the major source of lead at Rozelle, while a mixture of automotive and industrial sources is likely at Mayfield. The seasonal variation in the ratio of fine particle to TSP lead may be due to the higher humidity during the summer months: this should favour aggregation of small airborne particles to form larger ones.

A compilation of ERDC project data and EPA data for the Lidcombe site during 1992 is given in Figure 5.23. Both lead and bromine concentrations are higher during the winter than the summer months. However, the mass ratio of Pb/Br does not remain constant: during summer the ratio may rise to 6, while in winter it is close to the 2.1 (the value expected on the basis of the Pb and Br content of petrol sold in the Sydney area). This seasonal pattern is found at all the Sydney sites. If it is assumed that the major source of fine lead measured in the Sydney area is motor vehicles, these results imply that during the summer months approximately two-thirds of the bromide ions are lost from the aerosol. This loss from lead aerosols during the summer has been frequently reported in the literature (Biggins and Harrison, 1979) and can occur as a result of conversion to hydrogen bromide or elemental bromine.

Loss of hydrogen bromide could occur as a result of strong acids present in the aerosol. During the summer months in Sydney, there is evidence for an increase in rainwater acidity, (Ayers et al., 1987). The increase in aerosol acidity during summer may be due to the production of nitric acid and organic acids as a result of photochemical processes, and to a decrease in the extent of acid neutralisation by basic compounds (eg. metal oxides and carbonates) in the atmosphere. There is a decrease during summer in the concentration of bivalent and trivalent cations associated with basic compounds (Figure 5.23(e),(f)), in agreement with earlier findings (Ayers et al., 1987) and correlated with a decrease in nitrogen oxide concentrations from combustion sources (Figure 5.23(i)). Potassium salts (eg. potassium carbonate from wood ash) are also lower (Figure 5.23(g)). Non-seawater sulphate concentrations in fine-aerosol particles at Lidcombe remain approximately constant throughout the year (Figure 5.23(d)). The quantity of sulphuric acid added to the aerosol must therefore remain constant, though the extent of its neutralisation may vary with the season. At other sites in the ASP network, significantly greater concentrations of non-seawater sulphate were observed during the summer months. This pattern has been reported frequently overseas and attributed to the more rapid oxidation of sulphur dioxide to sulphuric acid in photochemical smog; it has also been used to explain the increase in aerosol acidity during the summer months, leading to loss of hydrogen bromide (Biggins and Harrison, 1979). Little information is yet available on the concentration of ammonium ions in

## **5.5 ELEMENT RATIOS AS INDUSTRIAL INDICATORS**

Elements which are uncommon in nature are sometimes released during industrial processes; under favourable conditions, they may be used as indicators for one process or a group of related processes. The reliability of an indicator species may often be improved by taking its ratio with another element to which it is related. The following ratios are a few which have been examined and may prove useful in the future.

### **5.5.1 Cobalt / iron**

Cobalt is rare in nature, but used extensively in steel making. Cobalt and iron concentrations near iron smelters at Mayfield and Warrawong are highly correlated during the first half of 1993 (Figure 5.24). This ratio may prove valuable for distinguishing the iron from steel making processes from the iron arising from other sources, such as soil and ash.

### **5.5.2 Vanadium / carbon**

Vanadium occurs in ancient porphyry structures which remain in the 'organic matter' of fossil fuels. It is ubiquitous in soils and in natural airborne particles but at very low levels. If combustion of fossil fuel leads to the release of airborne ash particles, it is expected that detectable quantities of vanadium may be present. If combustion is incomplete, elemental carbon will also be present. It was found that vanadium and elemental carbon were correlated at Warrawong during the first six months of 1992-3 (Figure 5.25). This ratio may prove useful as an indicator of incomplete fossil fuel combustion.

### **5.5.3 Iron / sulphur**

The relationship between iron and sulphur varies with the site (Figure 5.26). At Mayfield, a linear relationship exists, but there is a significant value for the x-intercept, implying the presence of sulphur unrelated to steel making activities. This indicates other sulphur sources. At Warrawong, the relation is again linear with a small y-intercept, which is probably insignificant. At other sites such as Muswellbrook, there is no correlation between the two elements. The ratio may prove useful as a metallurgical indicator.

## 6. CONCLUSIONS

With funding from the Energy Research and Development Corporation (ERDC) a fine aerosol sampling network was established in an area covering 60,000 square kilometres of New South Wales. The network consisted of 24 sampling units monitoring the major population areas of Wollongong, Sydney and Newcastle, and one unit at the global baseline station at Cape Grim in northwest Tasmania. The network commenced sampling in July 1991 at 3 sites in Sydney, and by the end of February 1992 all sites were providing data. Each site operated every Wednesday and Sunday providing two filters a week for analysis of fine (PM<sub>2.5</sub>) particles. More than 5000 filters were analysed, each for more than 20 different elements ranging from hydrogen to lead.

Between January 1992 and June 1993 over 5000 samples were collected and analysed, each for more than 20 different elements ranging from hydrogen to lead. The success rate for sampling and analysis was over 97%, and the project has produced a database of over 150,000 chemical measurements on fine particles. An effort is being made to obtain meteorological data at or close to 20 of the 25 sampling sites so that the interpretation of pollution events can be improved.

For this study, elements have been combined into a few major components to represent major constituents of the aerosols, which in conjunction with some tracer elements have been used to 'fingerprint' important sources. These parameters include: the total fine particle weight, 'ammonium sulphate', 'organic matter', 'soil', 'soot', 'salt' and elements such as potassium, iron, copper, zinc, bromine and lead. The trace element potassium is indicative of smoke from wood burning, combustion processes and bushfires; iron and copper can be used to identify industrial processes such as metal smelting and steel manufacturing, while bromine and lead can be used as a tracer for motor vehicles and industry.

The monthly average concentrations of these components, together with the elemental concentrations for each of the 25 ASP sites are given in Appendix 1 and 2 of this report. The 1992 average concentrations of elements for PM<sub>2.5</sub> particles for all sites in the network are listed in Table 6.1.

The average total fine particle mass for the ERDC network was 7.7µg/m<sup>3</sup>, and on average consisted of 23% 'organic matter', 23% 'ammonium sulphate', 23% elemental carbon, 7% 'salt', 6% 'soil', 1% lead, with the remainder being trace elements, water and nitrates. The five highest and five lowest average fine particle concentrations of major components and elements for each site are listed in Table 6.2.

**Table 6.1** Average concentrations of elements for PM<sub>2.5</sub> particles for all sites in the network, 1992

Element	Average concentration (ng/m <sup>3</sup> )	Percent by Weight (%)	Element	Average concentration (ng/m <sup>3</sup> )	Percent by Weight (%)
H	269	3.5	Mn	5.8	0.1
Na	212	2.8	Fe	71	0.9
Al	33	0.4	Co	0.5	<0.1
Si	58	0.8	Ni	0.5	<0.1
P	6.6	0.1	Cu	2.0	<0.1
S	429	5.6	Zn	17	0.2
			Br	33	0.4
Cl	268	3.5	Pb	88	1.2
K	52	0.7	Soot	1735	23
Ca	25	0.3	'Soil'	434	5.7
Ti	2.8	<0.1	(NH <sub>4</sub> ) <sub>2</sub> SO <sub>4</sub>	1769	23
V	0.4	<0.1	Smoke	9.0	0.1
Cr	0.5	<0.1	Organics	1780	23

The industrial site of Mayfield in the Newcastle area had the highest average fine particle concentration in 1992 (12.2µg/m<sup>3</sup>), followed closely by four metropolitan Sydney sites: Pyrmont, Mascot, Rozelle and Lidcombe. The major difference between Mayfield and the four Sydney sites was in the 'soil' component, which at Mayfield was higher by a factor of two. In the Illawarra region the highest yearly average total mass was measured at Warrawong (9.8µg/m<sup>3</sup>). The total fine particle mass fell from 10-12µg/m<sup>3</sup> for inner city sites to around 6µg/m<sup>3</sup> at sites 200 km from the city. Crookwell, in the southwestern region of the network, had the lowest yearly average fine particle mass in 1992, (3.5µg/m<sup>3</sup>).

The average concentration of sulphur in fine particles for all sites was 0.44µg/m<sup>3</sup>, with values in summer being generally 2 to 5 times higher than wintertime concentrations.